



DEPARTMENT OF INFORMATICS

TECHNISCHE UNIVERSITÄT MÜNCHEN

Master's Thesis in Data Engineering and Analytics

Analyzing Performance Bottlenecks in Collaborative Deep Learning

Adrian David Castro Tenemaya





DEPARTMENT OF INFORMATICS

TECHNISCHE UNIVERSITÄT MÜNCHEN

Master's Thesis in Data Engineering and Analytics

Analyzing Performance Bottlenecks in Collaborative Deep Learning

Analyse von Leistungsengpässen im Kollaborativen Deep Learning

Author:	Adrian David Castro Tenemaya
Supervisor:	Prof. Dr. Ruben Mayer
Advisor:	M. Sc. Alexander Isenko
Submission Date:	November 15, 2022



I confirm that this master's thesis in data engineering and analytics is my own work and I have documented all sources and material used.

München, November 15, 2022

Adrian David Castro Tenemaya

Acknowledgments

Thanks to everyone who tagged along on my academic journey. A special thanks go to my wonderful and supportive parents Laura and José; my “sore” Valeria, and my girlfriend Iris. Also, thanks to everyone who has believed in me and who didn’t make me quit (you know who you are). Finally, many thanks to my very patient academic advisor Alexander.

ABSTRACT

The amount of computing resources required to train state-of-the-art deep neural networks is steadily growing. Most institutions cannot afford the latest technologies, which are sometimes needed to keep up with today’s demanding deep neural network research. Access to powerful devices is therefore limited to a few parties. To tackle this, distributed training techniques such as volunteer computing can be employed.

Hivemind [tea20] is an open-source framework that enables collaborative model training using a large number of heterogeneous devices from universities, companies, and volunteers. In Hivemind, every device participating in the computation may differ in its characteristics, featuring different architectures and network speeds. The authors performed an interactive demonstration of collaborative computing with 40 volunteers, training a modified version of DALL-E [Ram+21] neural network model over 2 months. The reported results, however, do not include information about the effects of different Hivemind configurations on training.

In this thesis, we focus on the effects of training ResNet18 [He+15] on Imagenet-1k [Den+09] with Hivemind when using the parameter averaging algorithm [Dis+21] compared to regular training. We evaluate the effect of several aspects of training with Hivemind in a controlled cluster setup through 288 synthetic experiments. Each experiment uses different training and Hivemind settings such as the number of peers involved in the training, using local updates, batch size, learning rate. We show that training with Hivemind can be beneficial in terms of training time in specific scenarios and settings compared to regular training with a single node. Finally, we provide some considerations and lessons learned by summarizing the results of our experiments.

Contents

Acknowledgments	iii
ABSTRACT	iv
1 INTRODUCTION	1
1.1 Motivation	3
1.2 Approach	4
1.3 Contributions	5
2 FUNDAMENTALS	6
2.1 Neural Networks	6
2.1.1 Training	8
2.1.2 Gradient Accumulation	8
2.2 Distributed Computing and Storage for Neural Networks	9
2.3 Distributed Training	10
2.3.1 Bottleneck Analysis	12
2.3.2 Metrics	12
2.4 Hivemind	13
2.4.1 Decentralized Hash Table (DHT)	13
2.4.2 Optimizer	13
2.4.3 Parameter Averaging	15
3 RELATED WORK	19
3.1 Data Parallelism	19
3.2 Large Batch Training	19
3.3 Volunteer Computing	20
4 SETUP	21
4.1 Experimental Setup	21
4.2 Metrics	22
4.3 Implementation	24

5	EXPERIMENTS	26
5.1	Base Case	26
5.2	Not-Baseline Case	27
5.3	Metrics comparison framework	29
6	RESULTS	31
6.1	Baseline runs	31
6.2	Focus on effects of batch size, learning rate and target Batch Size	35
6.3	Focus on effects of gradient accumulation	39
6.4	Focus on effects of local updates	41
6.5	Focus on effects of the number of peers and vCPUs per peer	42
7	FUTURE WORK	48
8	CONCLUSIONS	50
	List of Figures	51
	List of Tables	53
	Bibliography	54

1 INTRODUCTION

It is safe to say that the internet paved the way for many things for humanity. Media such as images, video and audio can be shared across websites and applications, knowledge can be stored on faraway servers. This knowledge can then be retrieved with ease in text format using mobile devices, and products and services can be bought with the click of a button or a tap on a screen. Interactions, media and information make up for massive amounts of data that flow through complex computer systems, which in turn generate even more data and information.

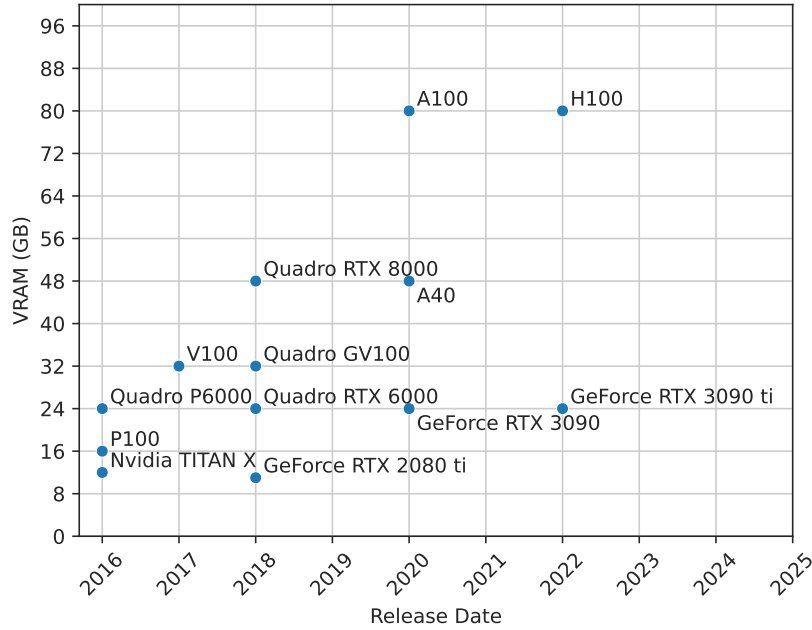
Researchers have found ways to leverage the magnitude of data that is being produced every second by countless systems all around the world. One of the most recent and most popular uses of this huge variety and quantity of data is deep learning.

Recently, models such as BERT [Dev+18], DALL-E [Ram+21], GPT-3 [Bro+20] and others have become incredibly popular thanks to their outstanding results and endless possibilities. DALL-E for example can generate high-quality realistic images and art starting from a text description written in natural language. These models however require massive amounts of data as well as very expensive computational resources, such as graphical processing units and tensor processing units (TPUs). In recent years, the size of neural network models has been steadily increasing exponentially, as shown by Figure 1.2. A simple calculation shows that the neural network model Megatron-Turing-NLG 530B [Smi+22] would take roughly $530 \times 4 = 2120\text{GB}$ of memory to simply hold its 530 billion weights.

Training a neural network model requires even more memory. Intermediate computation outputs such as gradient and optimizer states sometimes require 2 or 3 times as much memory than just the model parameters, making GPU memory one of the main bottlenecks in training huge neural network models. While some of these issues can be tackled using techniques such as parameter quantization [LTJ20], pruning and compression, they must not be considered one-fits-all solutions. Some models are simply too big to be trained on a single device. This problem is exacerbated by factors such as high GPU prices and much slower growth of their memory size relative to model size. Figure 1.1 shows the increase of GPU memory from 2016 to 2022.

To tackle these issues, practitioners studied and developed distributed computing techniques to train models that do not fit entirely in a single GPU’s memory, distributing the training load to potentially thousands of devices. Data parallelism has been widely

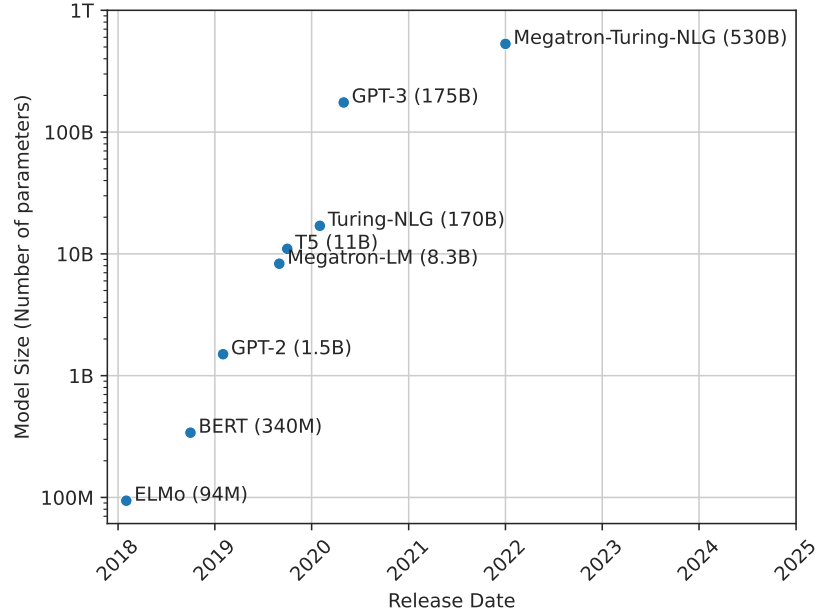
Figure 1.1: GPU VRAM over the past 4 years. The growth is mostly linear, doubling



adopted in the scientific community to train big models using paradigms such as parameter servers [Li+14a; Li+14b] and federated learning [Li+19a]. Both paradigms have difficulties when dealing with heterogeneous computing nodes such as straggler nodes, synchronization and weight stalenes. Because of this, researchers generally have to rely on massive amounts of resources and money to perform experiments and train their models using a set of homogeneous devices. This has become a problem for universities and small companies that want to train the models described in these papers, as they do not necessarily have access to such vast amounts of resources. Another problem is that practitioners may need to train models from scratch due to the incompatibility of their datasets with pre-trained ones, which are often trained on the most common datasets such as Imagenet [Den+09] and Fashion-MNIST [XRV17].

Volunteer computing is a paradigm in which people and institutions donate their idle computing resources such as laptops and other personal devices to solve hard problems. Historically, this technique has been used to distribute hard and complex problems such as Folding@Home [Beb+09], providing 2.43 exaflops of speed during the 2019 COVID pandemic. However, training neural networks using volunteer computing brings many challenges. Distributing optimization algorithms such as SGD and ADAM is challenging when dealing with heterogeneous devices. Participating peers may

Figure 1.2: Model size over the past 4 years, in logarithmic scale: ELMo [Pet+18], BERT [Dev+18], GPT-2 [Rad+19], Megatron-LM [Sho+19], T-5 [Raf+19], Turing-NLG [Mic20], GPT-3 [Bro+20], Megatron-Turing-NLG [Smi+22]



drop out during training or AllReduce operations such as optimizer and model state averaging, causing issues for the whole training network. Also, volunteer hardware may not be powerful enough to make a substantial difference in training, and in fact, their results may be discarded due to the inability of keeping up with more powerful peers.

Hivemind [RG20a] is a framework that enables volunteer computing across the internet for neural network training. In this thesis, we will analyze several aspects of training deep neural networks in a collaborative setting.

1.1 Motivation

Hivemind implements two fundamental training algorithms, Moshpit SGD [Rya+21a] and DeDLOC [Dis+21]. Moshpit SGD focuses on dealing with peers that may drop out during training, excluding their collaboration from the calculation if they become unavailable or unreliable. The focus of DeDLOC is instead on adapting the roles of participating volunteers depending on the current state of training. Hivemind

allows enabling several other distributed training features, such as large batch training [Goy+17] and controlling when averaging steps should be performed. The authors experimented with the tool in a real-life scenario by training a modified version of DALL-E [Ram+21] with 40 peers for two months [RG]. Most of the participating peers have donated their computing power through free resources such as Google Colab or their own hardware.

Although Hivemind was designed with internet training in mind, it can still be used to train neural networks within the perimeter of a single institution in controlled environments. We think that Hivemind can help researchers leverage their currently available hardware to perform training on large neural networks, instead of buying new and more expensive hardware.

To do so, we would like to answer the following research questions:

- Is it worth to setup and using low-power devices for training with Hivemind?
- Is adding more nodes to the computation always good, given the same amount of computational power in total?
- What is the effect on accuracy and training of increasing the number of gradient accumulation steps?
- What is the effect on accuracy and training of enabling Hivemind local updates?

In this thesis, we show that training with Hivemind in a controlled environment using limited and less powerful resources is still possible, with a few caveats and tuning.

1.2 Approach

To answer the questions above, we created 288 experiments performed on ResNet18 [He+15] model trained on Imagenet-1k [Den+09] and compile a lessons-learned section. In this thesis, we will compare regular training using a single node with 16vCPUs to training using Hivemind with multiple peers, where the sum of vCPUs per peer always amounts to 16. Also, we use a limited sample budget for every experiment of 320,000 samples in total split across the participant nodes or rounded up to the nearest digit if the number of samples cannot be precisely split. We compare training with key Hivemind settings, namely:

- batch size (BS);
- learning rate (LR);

- number of peers involved in the training (NoP);
- target number of samples that must be globally reached by all peers to perform an averaging round (TBS);
- number of steps to accumulate gradients for before calling the optimizer step (GAS);
- applying the gradients at every step or accumulating them until the next averaging round using Hivemind (LU);

As we test the software and its limitations, we might find possible areas of improvement in Hivemind. Whenever possible, we will further contribute using the knowledge gathered through our experiments by improving the Hivemind [tea20] source code.

1.3 Contributions

Our contributions are summarized as follows:

- We analyze the challenges of distributed training using Hivemind and provide insights on possible improvements.
- We verify the effectiveness of Hivemind for different peer hardware configurations.
- We use the gained knowledge and insights to contribute to the Hivemind open-source library.

2 FUNDAMENTALS

In this chapter, we are going to define the basic concepts needed to understand the contents of this paper. The mathematical details of algorithms or technical implementations of the presented technologies will not be described in depth, but rather briefly and concisely describe how they work.

@isenko: still working on this part!

We will formally define what are neural networks and how training works using a simple scenario. Following, we will introduce why and how distributed computing techniques are important in today's world, and how they can be used to facilitate neural network training. The topic of distributed neural network training is then presented. Finally, we describe Hivemind, how it works, why we chose this framework, which type of analysis we are going to conduct, and what kind of parameters are we focusing on in this paper.

2.1 Neural Networks

Neural networks (NNs) have been a major research area in the past decade. However, the basics of NNs as we know them today have been around for almost 70 years but did not gain much recognition until the 2010s. This is mostly because the success and viability of NNs are affected by two major factors, data availability and computational power, both of which were scarce or not advanced enough. As network-connected devices like smartphones and laptops started to become more widespread, the data that could be generated and gathered grew by several orders of magnitude. Today, NNs are used in many fields, from pharmaceutical to translation, from art generation to autonomous driving.

Let us introduce a simple example to support the following explanations. We might want to classify many images of cats and dogs using a NN so that its inputs are images of cats or dogs, and the output is a binary variable indicating 0 if the image is a cat and 1 if it is a dog.

To understand NNs, we have to look at their smallest components called *neurons*, which are functions that can be defined as follows:

$$y = g(X \cdot W + b) \tag{2.1}$$

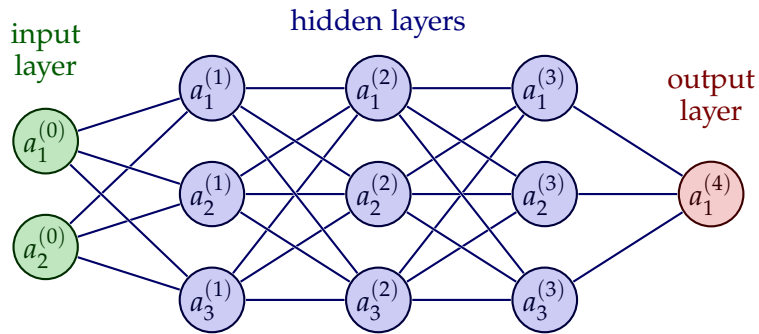
where g is called the activation function, $X \in \mathbb{R}^n$ is the neuron's input, $y \in \mathbb{R}$ is the output, $W \in \mathbb{R}^n$ its weights or parameters, and $b \in \mathbb{R}$ its bias. Note that activation functions must be non-linear functions. We would like to use NNs to solve and predict non-linear problems such as our example, a task that can only be achieved by using non-linear functions. If we were to compose a neural network using only linear functions, the output would still be a linear function, regardless of a NN's complexity. Examples of non-linear functions commonly used inside NNs are the sigmoid and the rectified linear unit (ReLU). The weights W and the bias b define the result of the activation function g .

The first and most simple type of NN that was devised is called *feed-forward neural network* (FF) and is comprised of many neurons stacked together in *layers*. These layers f are then composed together to form a feed-forward NN:

$$Y = f_1 \circ f_2 \circ \dots \circ f_L \quad (2.2)$$

where L is called the *depth* of a FF neural network, or number of *hidden layers* in a FF network.

Figure 2.1: An example of a neural network, with input layers (green nodes), hidden layers (blue nodes), and output layer (red node).



The depth, as well as the types of layers and functions of a given neural network, define its *architecture*. A NN architecture can be changed to obtain different results in terms of effectiveness, speed or other criteria. An example of one such architecture is represented in Figure 2.1.

At this point, the model has fixed parameters W and b , so given the same input, the output will be the same. We would like to update the parameters in such a way that the output reflects some arbitrary characteristic of the input, a process called *training*.

2.1.1 Training

Using our example, the NN should learn over time and using many examples, which images represent a cat, and which ones represent a dog. We can provide information to the neural network about whether or not it is right or wrong, and update its parameters according to how much it is far from the truth.

Formally, the function determining how much a NN is wrong about a guess is called a *loss function*, which outputs a value called *loss*. For a binary value such as our example, we can use the *binary cross entropy* loss function. The lower this value is, the closest the NN is to the ground truth.

We can derive certain properties from this value, such as how much should we change the parameters of our NN model so that we get a lower value the next time we try. This approach can be formally described as an optimization problem, where the optimization function, also called optimizer, is defined as follows:

$$\arg \min_{W,b} \mathcal{L}(W,b) \quad (2.3)$$

The optimizer function defines how the values of W and b should change to get a better loss. The process of iteratively updating these values multiple times using different inputs is called *training*. Commonly used optimizers for NN training are *Stochastic Gradient Descent*, *Root Mean Square* (RMSProp), *Adam* and others.

The values obtained using these optimization functions are used to determine the best next local optima for the given parameters. This process can then be repeated multiple times until an arbitrary loss value is reached, and the training process is stopped. The final architecture of the neural network and the state of the weights and biases are then fixed, obtaining the final NN model.

At several stages during training, a neural network practitioner might want to validate the results obtained by using a set of data that is different from the one that has been used to train the NN. This is called the *validation step*, and it is performed without changing the network's parameters or architecture. Validation steps are crucial to understanding if the changes made to a model are biased towards a specific set of inputs, an effect denominated *underfitting*.

2.1.2 Gradient Accumulation

When training neural networks, increasing batch size can sometimes lead to faster convergence [Kri14; Goy+17; YGG17]. However, simply increasing the batch size during training does not scale very well, and can lead to memory issues or an inability to train at all. To help simulate bigger batches on a single device without incurring these issues, we can use a technique called *gradient accumulation*.

Algorithm 1 shows a simplified version of an algorithm used to train neural networks. A dataset consisting of a set of inputs X and Y labels, both with length N , is used as the input to the model, with a training loop supporting a single epoch.

Algorithm 1 Standard training algorithm, PyTorch style

Require: $N \geq 0$

$X \leftarrow [\dots]$

▷ Inputs

$Y \leftarrow [\dots]$

▷ Labels

$i \leftarrow 0$

while $i < N$ **do**

$prediction \leftarrow model(X[i])$

$loss \leftarrow criterion(prediction, Y[i])$

$loss.backward()$

$optimizer.step()$

$optimizer.zero_grad()$

$i \leftarrow i + 1$

end while

Algorithm 2 shows a modified version of Algorithm 1 with gradient accumulation turned on. This technique introduces an accumulation variable (ACC) instructing how many batches should be accumulated within the optimizer's state. The $loss$ value is normalized with the value of ACC to account for the effects of the accumulation. Once ACC batches have been aggregated or when we have finished training, we apply the averaged gradients using the optimizer's function $optimizer.step()$, and reset its gradients to zero.

2.2 Distributed Computing and Storage for Neural Networks

A distributed system is defined as a system where its components communicate with one another using messages. In computer science, the use of distributed systems has been a field of research for many years and has boomed with the advent of network communications. We often see distributed systems in complex applications such as the backend of a website or supercomputers. These systems are often composed of tens or hundreds of connected components that collectively produce one or more outcomes, such as web pages or complicated simulations. Using distributed techniques is essential for these complex applications, as the computational load and complexity required to run them, are simply too great for a single machine.

The elevated number of components that make a distributed system can lead to several issues, such as an immense amount of requests to their local storage and

Algorithm 2 Training with gradient accumulation, PyTorch style

Require: $N \geq 0$ **Require:** $ACC > 0$ $X \leftarrow [...]$

▷ Inputs

 $Y \leftarrow [...]$

▷ Labels

 $i \leftarrow 0$ **while** $i < N$ **do** $prediction \leftarrow model(X[i])$ $loss \leftarrow criterion(prediction, Y[i])$ $loss.backward()$ $loss \leftarrow loss / ACC$ **if** $((i + 1) \bmod ACC == 0)$ **or** $((i + 1) == N)$ **then** $optimizer.step()$ $optimizer.zero_grad()$ **end if** $i \leftarrow i + 1$ **end while**

extremely large files. For these reasons, it is necessary to use storage solutions that can handle these kinds of stress. Several distributed storage solutions have been developed and adopted over the past years, each of them excelling in different solutions and lacking in other areas. In general, choosing the right distributed storage software is crucial, as it can mean the difference between loading a dataset in seconds or minutes.

Neural networks have quickly become too large in terms of memory and computationally expensive for a single host, thus needing distributed system techniques for training.

2.3 Distributed Training

Training a state-of-the-art neural network nowadays requires enormous amounts of time and effort, but especially resources and money. It is often impossible to train a model within the boundaries of a single piece of hardware, even with powerful specifications. This affects the speed at which neural networks are being developed and the ability to reproduce results from state-of-the-art models.

One of the first and most notable examples of the results of this phenomenon is AlexNet [KSH12], in which the authors mentioned the need of using more than one GPU to train their model. This was 2010, and a little more than a decade later, to train the newest neural network models, practitioners, companies and research institutes

need thousands of powerful GPUs. Distributed system techniques are used to be able to train these massive neural networks, creating the new term “distributed training”.

We briefly summarize distributed training techniques as follows:

- **Data parallelism;** given a set of n devices, an instance of the model is trained on each one of the devices. Usually, gradients obtained during backpropagation are then aggregated across all the devices using techniques such as *AllReduce*. This technique however does not work very well with models that exceed a single device’s available memory and is therefore used in applications with low-memory devices such as *Federated Learning* [Li+19b].
- **Model parallelism;** a deep neural network is conceptually split into n partitions across n devices, each hosting a different partition and set of weights. An early notable example of model parallelism is AlexNet [KSH12], where the authors decided to split the computation of some of the layers across two GPUs with 3GB of ram each, a concept illustrated in ???. This technique relieves the burden of a single node to host all of the weights of a model but is also more sensitive to issues with communication across nodes.
- **Pipeline parallelism;** a combination between model parallelism and data parallelism. Pipeline parallelism for machine learning models has been introduced in 2018 [Hua+18]. With this technique, each batch is split into micro-batches and sent to available computing devices such as GPUs, which individually compute both the forward and backward pass for that micro-batch. Finally, weights are averaged after backpropagation has taken place on every GPU.
- **Tensor parallelism;** tensor operations for huge neural network models can become a bottleneck, as they can require more memory than the host’s device can handle and can become slow in general. Tensor parallelism can alleviate a single node’s computational burden by splitting a tensor operation across many devices. This technique has been first introduced in neural network models in [Dea+12b] with a framework called DistBelief.
- **Mixture-of-Experts.** Instead of conceptually splitting a model, we construct multiple, different models and split them across workers, also called “experts”. A gating function helps each of the experts to specialize in a different subset of all training cases. The broader concept has been first introduced in 1991 [Jac+91] but has recently gained traction due to its flexibility in solving natural language problems.

The list is always evolving, and new techniques may be developed in the next years.

2.3.1 Bottleneck Analysis

By definition, a *bottleneck* is a component of a system that negatively affects the output of such a system. An example is reading and writing data from one system to another, where the storage on both sides is a very fast SSD (Solid State Drive), and the transmission speed that the network allows is 56KB/s. In this scenario, even if both systems could theoretically reach unlimited speeds in both read and write operations, the performance of the system is ultimately limited by the low transmission speed.

Most real-life cases however are not so simple, and the component or components that might act as the bottleneck of a system cannot as easily be detected as the previous example. It is necessary then to perform an analysis of all components of the system to establish its bottlenecks.

Systems can be very complex, and performing an analysis of all of their components may become very difficult or impossible in practice. Thus, we have to analyze a limited number of components at a time, starting with the most significant. Systems can also be dynamic. In certain cases, bottlenecks can be found on a certain subset of components, and in other cases, other components act as bottlenecks instead. This requires constant monitoring of key metrics of these components and an understanding of which metrics might be relevant and why.

2.3.2 Metrics

Metrics represent the raw information about the behavior of a system and its component, collected via a monitoring system. In the previous paragraphs, we have presented a relatively simple example of how bottlenecks can be identified by their components and their characteristics. However, the final identification of the bottleneck was given to us by our pre-existing knowledge of the system and its specifications. In complex and evolving systems, having pre-existing knowledge about their components is not always possible.

It is possible to gather metrics about information that is available via common interfaces such as operating system hooks and methods. We may track metrics about the host system such as:

- **disk space utilization**; in addition to the amount of storage used over time, we can also track read and write operations in terms of speed.
- **cpu utilization**; can provide insights about possible efficiency issues within the software by highlighting peaks in CPU utilization.
- **network utilization**; distributed systems in particular may benefit from tracking metrics about network utilization, as it is one of their main components.

- **memory utilization**; sometimes processes do not perform proper cleanup of their resources, leading to memory leaks, slowdowns and errors.

2.4 Hivemind

Hivemind is a framework that aims to enable decentralized training using several techniques, such as decentralized parameter averaging or decentralized mixture-of-experts. The initial concept of developing Hivemind was to enable neural network training outside the boundaries of an institution’s internal network and resources, such as universities and small-medium companies. These institutions do not necessarily have access to the latest technologies and hardware to keep up with big companies’ large budgets. By using Hivemind, it may be possible to collectively contribute to training neural networks across different institutions, unlocking new areas and possibilities of research.

In this section, we will introduce on a high level the main components and settings that we will use throughout the thesis.

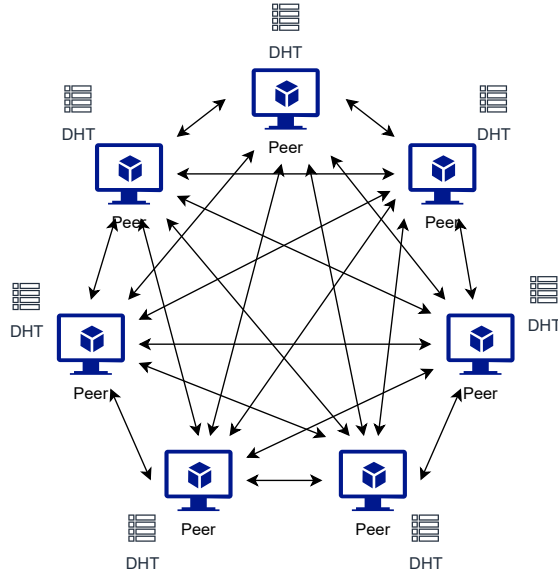
2.4.1 Decentralized Hash Table (DHT)

A decentralized hash table or DHT is a system that provides a set of features similar to a hash table in a distributed environment. Because Hivemind focuses on providing a training environment for nodes across the internet, a DHT is a beneficial part of the architecture because of its fault-tolerant properties. Under the hood, Hivemind uses a DHT to track the presence or dropout of peers during training and to allow a direct exchange of data between them. An example of how this type of communication works is given in Figure 2.2.

2.4.2 Optimizer

One of the main components of Hivemind is the Hivemind Optimizer, which wraps around any other implementation of a `torch.optim.Optimizer`. Therefore, the Hivemind Optimizer can be used as a drop-in replacement in regular training operations. With default settings and with no other peer, the Hivemind optimizer is designed to perform exactly as the underlying `torch.optim.Optimizer` class. There are several options for tuning the Hivemind Optimizer, which affect how distributed training is performed across participating peers in a training run. We will briefly describe some of the settings that we focused on during this thesis.

Figure 2.2: Nodes in a Peer-to-Peer network exchanging data directly with one another. Every node has its own internal DHT which is kept in sync with other peers.



Target Batch Size

The target batch size (TBS) is defined in the Hivemind Optimizer as the global number of samples that every peer has collectively processed during a collaborative run in the current Hivemind epoch. A Hivemind epoch, which we will call *HE*, does not necessarily correspond to a full pass over the training data and can be used to synchronize advanced training features like optimizer schedulers. The HE starts at 0 at the beginning of training and increases by one every time that all participating peers reportedly finished processing *TBS* since the last *HE*.

Understanding the concept of HE is crucial, so let us describe a simple scenario to aid with this task:

- two peers are collaboratively training a model;
- the TBS is 256;
- the `use_local_updates` setting is set to True (see next section for a definition of this setting);
- each peer processes a batch size of 64;
- each peer processes every batch at roughly the same speed;

- each peer starts training at the same time.

After one step, the number of globally accumulated samples is equal to $64 + 64 = 128$, as each peer has processed the same amount of samples in the same amount of time. After another step, the accumulated samples are equal to $128 + (64 + 64) = 256$. Because the total number of accumulated samples is now 256 and it is equal to TBS, each peer can now initiate an averaging round with all other participating peers. What happens right before and after averaging depends on the `use_local_updates` setting.

2.4.3 Parameter Averaging

Optimizers used for deep learning training such as SGD [KW52] and ADAM [KB14] need some information stored in memory to operate. When training collaboratively, each peer may perform operations using a local version of these vectors to proceed with training. However, optimizer parameters may diverge during training, in turn causing the underlying model parameters to diverge. It is possible to mitigate this effect by performing operations that take into account all of the peer's information, for example with *AllReduce* operations. In the case of Hivemind, the operation of choice is averaging, which can be performed for both the optimizer state and the gradients before applying them to the model.

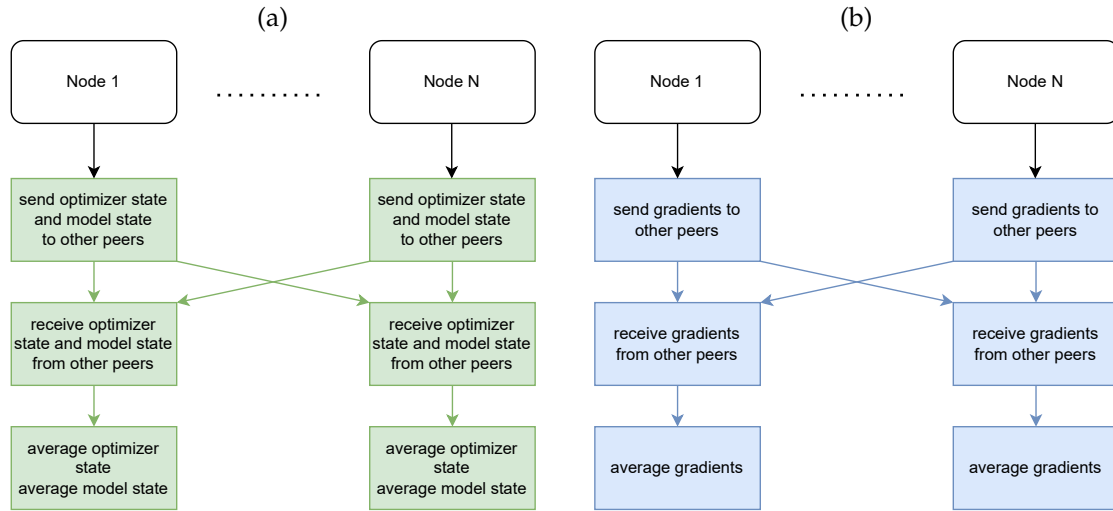


Figure 2.3: State averaging (left) and gradient averaging (right) in Hivemind.

Local Updates

Training neural networks with larger batches has been proven to be beneficial in some cases [Kri14; Goy+17; YGG17]. Thus, practitioners may want to be able to accumulate gradients either locally, in a distributed manner, or a combination of both. Hivemind’s implementation of distributed training extends the concept of gradient accumulation, previously presented in Subsection 2.1.2, by introducing the `use_local_updates` settings for `hivemind.Optimizer`.

The setting has two modes:

- **activated**; after every local training step, the Hivemind optimizer applies the gradients to the model. At the next HE, the final stage of the Optimizer starts. A simplified flow of how Hivemind implements this mode is illustrated in Figure 2.4.
- **deactivated**; after every local training step, gradients are accumulated instead of being applied to the model’s parameters. After *ACC* steps, the optimizer is invoked and internally stores the accumulated gradients. At the next HE, the Optimizer averages the accumulated gradients with all participating peers. The final stage of the Optimizer then starts, which averages the model and optimizer state with other peers. A simplified flow of how Hivemind implements this mode is illustrated in Figure 2.5.

In this thesis, we will discuss the effects of enabling or disabling this setting on training.

Figure 2.4: Diagram of Hivemind training with local updates enabled.

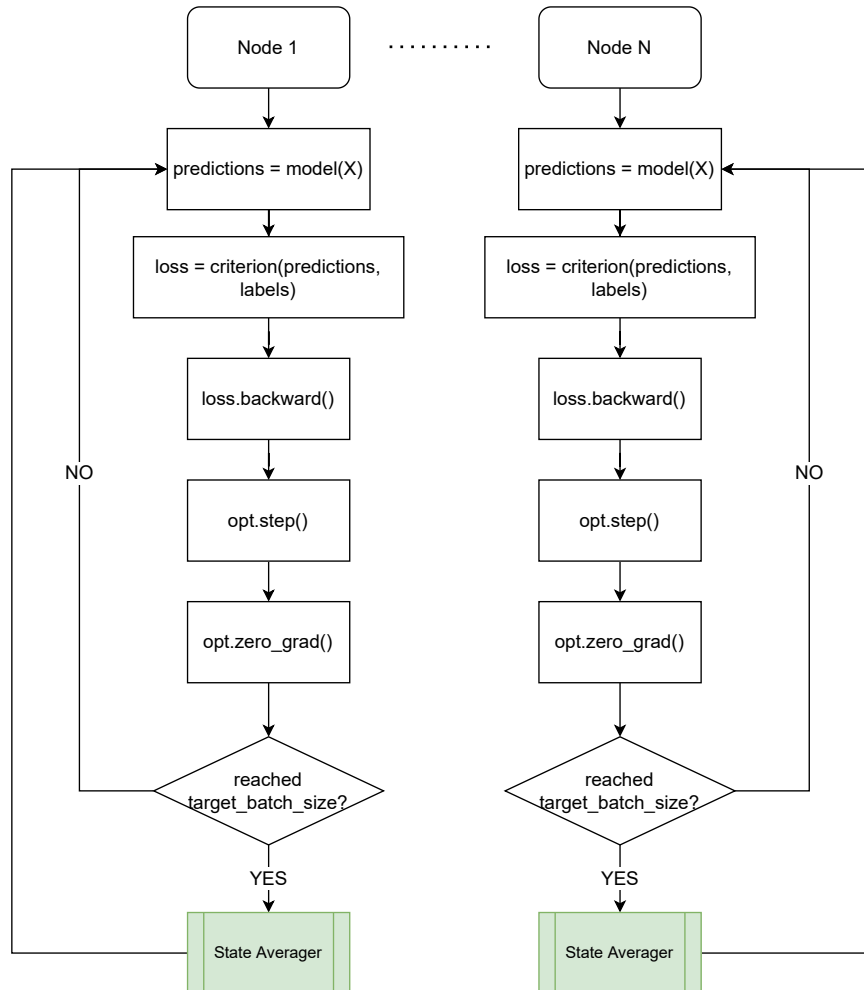
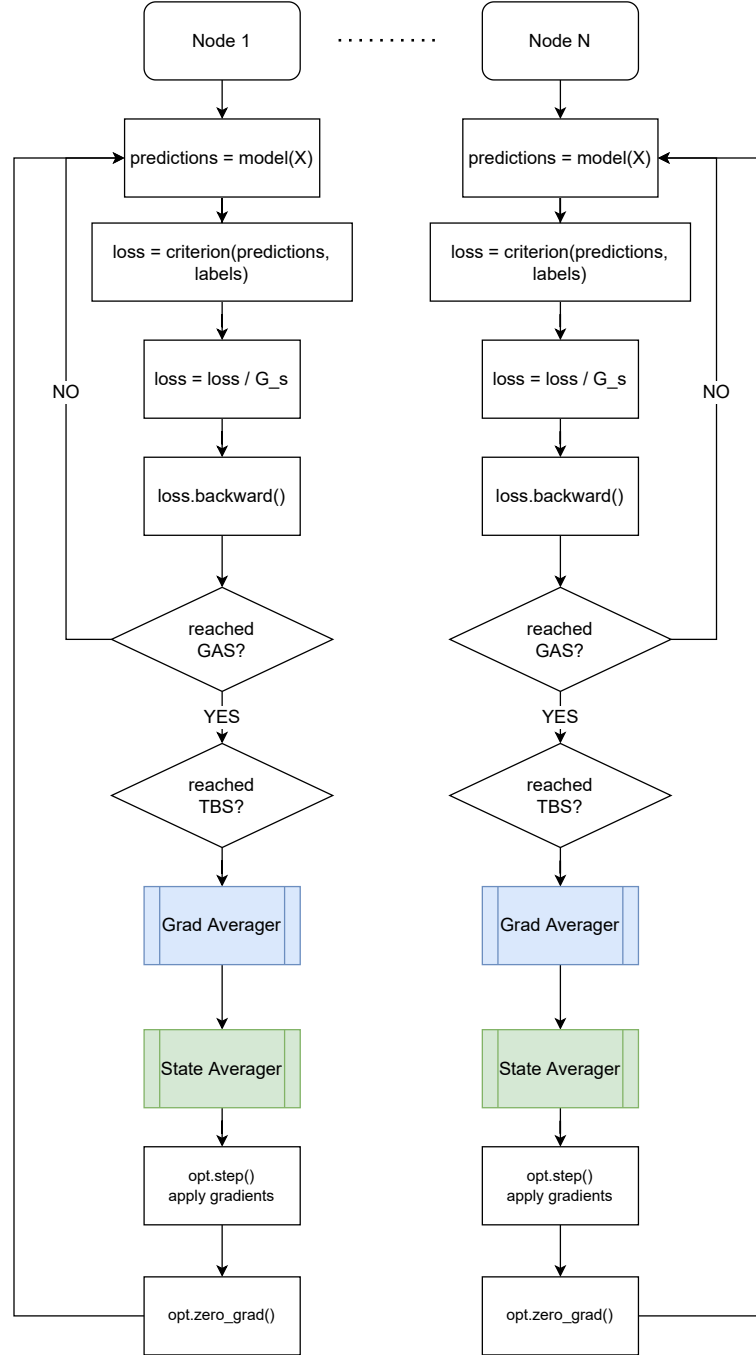


Figure 2.5: Diagram of Hivemind training with local updates disabled.



3 RELATED WORK

In this chapter, we provide the necessary background to understand this thesis and discuss related work.

3.1 Data Parallelism

Throughout the years, datasets and machine learning models have grown in size, requiring distributed techniques to train them efficiently. Data parallelism is the most common type of distributed learning and has been implemented on many common frameworks such as PyTorch¹ and TensorFlow² through a high-level API. It has been known however that operations such as updating and distributing large neural network models can run into network bottlenecks [HHS17; LTJ20; Dea+12a; Sha+18]. Because of this, operations such as pruning and quantization are common to reduce the impact of communication in a distributed training setting [Bla+20; HMD15]. Despite these efforts, increasing the number of nodes and model size can still cause network bottlenecks. Less known are the effects of preprocessing bottlenecks, which can severely affect the performance of models before training even starts [Ise+22; Xin+21]. In this thesis, we show a general approach for studying and evaluating the effects of bottlenecks in data parallelism using Hivemind.

3.2 Large Batch Training

Training neural networks using large or very large batches [Kes+16; HHS17] has gained traction amongst researchers. Using small batch sizes is generally preferable when using minibatch SGD algorithms as it allows escaping local minima within a few iterations. Increasing the number of minibatches also decreases the update frequency, making training faster. However, this also leads to the possibility of getting stuck on local minima due to less noisy updates and thus low training performance overall.

The attractiveness of using large batches is to leverage the parallelism properties of distributed optimization algorithms. Goyal et al. have managed to train Imagenet

¹<https://pytorch.org/>

²<https://tensorflow.org/>

in around 1 hour using a batch size of 8192 [Goy+17]. This was possible as they showed that the decrease in performance when increasing the minibatch size is highly non-linear, staying constant for values up until 8192 and increasing rapidly afterward. As training can still diverge in the first parts of training, they introduce a warmup period where a single node starts training, after which more nodes can join.

In their experiments, Riabinin et al. show that it is possible to perform large batch training in a volunteer computing setting using Hivemind [RG20b; Dis+21]. Hivemind allows setting different strategies for when parameters and model states are averaged, effectively simulating larger batches across participating peers. However, there is a limited amount of experiments showcasing different Hivemind configurations in a controlled environment.

3.3 Volunteer Computing

Researchers today are dealing with hard and complex problems such as particle simulation and protein folding. Because of their nature, these problems require immense amounts of computational power, which are not always available to single institutions. Supercomputers can help tackle these problems, but access to them is limited. In the early days of distributed computing, it was found that researchers could leverage the power of volunteers who donate their idle devices to help solve their problems. This paradigm is denominated *volunteer computing* (VC).

Standard data parallelism distributed algorithms are made with node reliability in mind, and a node failure may simply cause the whole training to fail. However, in VC, a node dropping off mid-training is an expected case. For these reasons, few works have successfully implemented VC for deep learning training. Most VC works use a server-client infrastructure, where the server is hosted and managed by the runners of the experiments and the clients are the volunteers [AJR21; MCA19]. The server in this case becomes a single point of failure and possible bottleneck, which can become an issue if an elevated number of volunteers joins the training.

The Hivemind framework [Rya+21b] uses a modified version of minibatch SGD [Rya+21b] that considers node failure. Furthermore, the authors implemented DeD-LOC, a dedicated training algorithm [Dis+21] that removes the single node of failure bottleneck. Hivemind has been proven successful in an experiment training a modified version of DALL-E [Ram+21] with 40 volunteers over two months.

4 SETUP

In this chapter, we briefly describe the technologies and resources that we have used to run our experiments, as well as how they were set up and provisioned. We further describe our experimental setup and the hyperparameters that we chose to experiment on. Finally, we present a high-level overview of our implementation with a simplified visualization.

4.1 Experimental Setup

All our experiments are trained using the model ResNet18 [He+15] on Imagenet-1k, with 1.281.167 items and 1000 classes [Den+09]. The optimizer function of choice is standard stochastic gradient descent (SGD) with three possible learning rate settings (0.1, 0.01, 0.001) and a fixed momentum value of 0.9.

To support our training experiments we used a cluster provided by the department of Decentralized Information Systems and Data Management, from the Technische Universität München. This cluster is managed by OpenNebula, and gives us access to several machines with Intel Xeon v3 8x@2.4 Ghz, 80 GB DDR4 RAM and Ubuntu 20.04 image. As the storage backend, we use a CEPH cluster backed with hard disks, with 10 GB/s up and downlink. We repeat every baseline experiment four times, and every hivemind experiment only one time. All experiments use Python 3.8.10, and Hivemind with the commit hash `de6b4f5ae835a633ca7876209f2929d069e988f0` ¹. We used the Infrastructure-as-Code (IaC) tool Terraform together with the OpenNebula provider 1.0.1 ² to spin up several virtual machines matching our needs.

The types of virtual machines that we used for this thesis are two:

- **messengers**; helps with establishing the initial connection between every bee. Does not produce or consume any data besides the initial connection step.
- **bees**; machines that participate in training a model. Bees can be executed with Hivemind turned on or off, the latter being the default setting when running

¹We chose this specific commit because we identified some issues with training on our setup from the next commit onwards

²<https://registry.terraform.io/providers/OpenNebula/opennebula/1.0.1>

baseline experiments. When executing with Hivemind on, bees connect to a single messenger machine for initializing their internal DHT and then proceed to communicate with one another for the rest of the experiments.

Every virtual machine spawned has 10GB of RAM and 30GB of internal disk space backed up by SSD, and they are all connected to the same CEPH storage backend presented earlier. Messenger machines always have one vCPU assigned to them by the underlying OpenNebula KVM. Depending on the experiment, bees can either be assigned with 16vCPUs, 8vCPUs, 4vCPUs, 2vCPUs or 1vCPUs.

It is worth noting that because of the nature of how a KVM assigns virtual CPUs to a virtual machine, the machines with 1vCPU may occasionally use more than one thread in case of long I/O waiting times. This causes metrics such as CPU utilization to go over 100%, although at all times always one core is utilized by the virtual machine. With our current setup, there is no way to go around this limitation.

To log our metrics, we decided to use the tool *Weights and Biases (wandb)*³. The impact of this tool on the logged metrics on Hivemind experiments is later considered when compared to baseline experiments.

4.2 Metrics

We logged key metrics from the host system of every machine using the Python tool *psutil*, which gives us access to the metrics listed in Table 4.1. Not every metric will be used and analyzed throughout this thesis.

Table 4.1: List of key host metrics logged using *psutil*.

Metric key	Description
bandwidth/disk_read_sys_bandwidth_mbs	bandwidth used by local disk read operations
bandwidth/disk_write_sys_bandwidth_mbs	bandwidth used by local disk write operations
bandwidth/net_sent_sys_bandwidth_mbs	bandwidth used by network send operations
bandwidth/net_recv_sys_bandwidth_mbs	bandwidth used by network receive operations
cpu/interrupts/ctx_switches_count	number of context switches that occurred since the last call
cpu/interrupts/interrupts_count	number of CPU interrupts that occurred since the last call

³<https://wandb.ai/>

4 SETUP

cpu/interrupts/soft_interrupts_count	number of soft CPU interrupts that occurred since the last call
cpu/load/avg_sys_load_one_min_percent	average CPU load across the last minute
cpu/load/avg_sys_load_five_min_percent	average CPU load across the last five minutes
cpu/load/avg_sys_load_fifteen_min_percent	average CPU load across the last fifteen minutes
cpu/logical_core_count	number of logical cores available to the current host
memory/total_memory_sys_mb	total amount of memory in megabytes available to the current host
memory/available_memory_sys_mb	amount of unused memory in megabytes since the last call
memory/used_memory_sys_mb	amount of used memory in megabytes since the last call
memory/used_memory_sys_percent	percent of memory used since the last call
process/voluntary_proc_ctx_switches	number of voluntary process context switches since the last call
process/involuntary_proc_ctx_switches	number of involuntary process context switches since the last call
process/memory/resident_set_size_proc_mb	resident set size in megabytes of the current process since the last call
process/memory/virtual_memory_size_proc_mb	virtual memory size in megabytes of the current process since the last call
process/memory/shared_memory_proc_mb	shared memory size in megabytes of the current process since the last call
process/memory/text_resident_set_proc_mb	memory devoted to executable code in megabytes since the last call
process/memory/data_resident_set_proc_mb	physical memory devoted to other than code in megabytes since the last call
process/memory/lib_memory_proc_mb	memory used by shared libraries in megabytes since the last call
process/memory/dirty_pages_proc_count	number of dirty pages since the last call
disk/counter/disk_read_sys_count	how often were reads performed since the last call
disk/counter/disk_write_sys_count	how often were writes performed since the last call
disk/disk_read_sys_mb	how much was read in megabytes since the last call

disk/disk_write_sys_mb	how much was written in megabytes since the last call
disk/time/disk_read_time_sys_s	how much time was used to read in seconds since the last call
disk/time/disk_write_time_sys_s	how much time was used to write in seconds since the last call
disk/time/disk_busy_time_sys_s	how much time was used for I/O operations in seconds since the last call

To monitor the effects of Hivemind on training, we also log at the end of every training step the metrics listed in Table 4.2

Table 4.2: List of key host metrics logged using psutil.

Metric key	Description
train/loss	Loss reached in the current step
train/accuracy	Accuracy reached in the current step
train/samples_ps	number of samples processed per second passed from the start of the current step until the end
train/data_load_s	time taken to load the current step batch in seconds
train/model_forward_s	time taken to perform the forward pass in seconds
train/model_backward_only_s	time taken to perform the backward pass in seconds
train/model_opt_s	time taken to perform the optimizer step in seconds
train/step	current step number

4.3 Implementation

To perform the experiments, we developed a custom solution that automates most manual steps using a combination of Ansible playbooks and bash scripts.

When setting up a new experiment, the following steps are performed:

1. copy configuration to all participating machines; this step includes the messenger machine, as well as the bee machines. This is to ensure that all machines are using the same code.
2. (only for Hivemind) start the messenger machine; the messenger acts as the first point of contact for all the machines, providing a common endpoint that they can connect to for establishing the initial connection.
3. run bees; there are two cases for this step: a) if step 2 was performed, bees are running using Hivemind. All bees run with the parameter `initial_peers` set to

the messenger's DHT address. b) otherwise, all bees are performing a baseline experiment, and no Hivemind feature is enabled.

5 EXPERIMENTS

Having access to more powerful hardware is a challenge for several reasons that may be outside of our control. In the past years, there was a worldwide shortage of microchips that negatively impacted the ability to purchase state-of-the-art hardware such as CPUs and GPUs. Thus, we would like to understand the effects of running distributed frameworks such as Hivemind on less powerful, older hardware.

To provide a fair comparison between experiments not running Hivemind and experiments that do, our experiments always have the same amount of vCPUs. Finally, every experiment processes the same number of samples across all the participating peers, and the sum of processed samples may never be greater than 320,000.

An exception to this rule is made for experiments with an odd number of samples per peer. For example, a run with batch size 128 and 8 peers should result in 312.5 samples per peer, which is not possible. In these cases, the number of samples per peer is rounded up to the nearest digit to form an even number. This chapter describes the basic setup of our experiments.

5.1 Base Case

To preserve a comparison consistency between each experiment run, the number of steps depends on two factors: the number of peers involved in the training, and the batch size. We designed our baseline experiments in a grid search, covering the following training hyperparameters:

- Batch Size (BS): 32, 64 and 128;
- Learning Rate (LR): 0.001, 0.01 and 0.1;
- Max Steps (MS): 10000 for BS=32, 5000 for BS=64, 2500 for BS=128.
- Gradient Accumulation Steps (GAS): 1 (no accumulation), 2 (with accumulation up to two steps)

Table 5.1: List of baseline experiments and hyperparameters

Baseline experiments			
Max Steps	Batch Size	Learning Rate	Grad. Acc. Steps
10000	32	0.001	1
10000	32	0.01	1
10000	32	0.1	1
5000	64	0.001	1
5000	64	0.01	1
5000	64	0.1	1
2500	128	0.001	1
2500	128	0.01	1
2500	128	0.1	1
10000	32	0.001	2
10000	32	0.01	2
10000	32	0.1	2
5000	64	0.001	2
5000	64	0.01	2
5000	64	0.1	2
2500	128	0.001	2
2500	128	0.01	2
2500	128	0.1	2

The machines used for baseline runs have 16vCPUs and each experiment is repeated 4 times to observe the reproducibility of the measurements. Hivemind features such as the DHT and the Optimizer wrapper are completely deactivated for these runs. Table 5.1 lists all the 18 combinations of experiments that we cover in this thesis.

5.2 Not-Baseline Case

To test and isolate the effects of using Hivemind for distributed training, every experiment changes only a single parameter at a time. For this, we can divide the set of non-baseline cases into different categories depending on which parameter has been changed. In every non-base case scenario described in this section, at least two nodes are involved in the training of the underlying NN model.

The model and the dataset remain the same across each run, and every peer has full access to the entire dataset through our CEPH cluster. We repeat the same experiments as the baseline runs, and further explore the following Hivemind settings and questions:

- **Number of Peers (NoP):** 2, 4, 8 and 16; for loads like the experiment that we are running, is communication between many nodes a bottleneck?
- **Number of logical cores per node (vCPUs):** 1, 2, 4, 8 and 16; using the same amount of computational power across many nodes, do we get to a target accuracy faster?
- **Target Batch Size (TBS):** 10000, 5000, 2500, 1250 and 625; using smaller target batch size, do we get faster to a target accuracy?
- **Max Steps (MS):** 5000, 2500, 1250 and 625; this parameter depends on the number of peers and batch size, but the total is always 320,000 steps per experiment;
- **Use Local Updates (LU):** True or False; Hivemind allows us to control when to schedule gradient, model and parameter averaging. How does this setting affect training?

The Table 5.2 shows a list of the combination of experiments that we performed to test Hivemind. In total, we have executed 288 experiments for this thesis.

Table 5.2: List of Hivemind experiments and hyperparameters. Every experiment has been executed once, and every time with at least two peers.

Experiments testing for the effect of target batch size (TBS)							
MS	NoP	vCPUs	BS	LR	TBS	GAS	LU
5000	2	8	32	0.001, 0.01, 0.1	10000, 5000, 2500, 1250, 625	1,2	T, F
2500	2	8	64	0.001, 0.01, 0.1	10000, 5000, 2500, 1250, 625	1,2	T, F
1250	2	8	128	0.001, 0.01, 0.1	10000, 5000, 2500, 1250, 625	1,2	T, F
Experiments testing for the effect of the number of peers (NoP)							
MS	NoP	vCPUs	BS	LR	TBS	GAS	LU
2500	4	4	32	0.001, 0.01, 0.1	1250	1,2	T, F
1250	8	2	32	0.001, 0.01, 0.1	1250	1,2	T, F
625	16	1	32	0.001, 0.01, 0.1	1250	1,2	T, F
1250	4	4	64	0.001, 0.01, 0.1	1250	1,2	T, F
625	8	2	64	0.001, 0.01, 0.1	1250	1,2	T, F
313	16	1	64	0.001, 0.01, 0.1	1250	1,2	T, F
625	4	4	128	0.001, 0.01, 0.1	1250	1,2	T, F
313	8	2	128	0.001, 0.01, 0.1	1250	1,2	T, F
157	16	1	128	0.001, 0.01, 0.1	1250	1,2	T, F

We have fixed the following Hivemind hyperparameters that were not the focus of

this thesis, although some can be further explored:

- **matchmaking_time**; defines for how many seconds the optimizer should wait for other peers to join an averaging round. We set this value to 10. Ideally, optimizers should never have to wait for this long amount of time in our setup.
- **averaging_timeout**; after this many seconds, an averaging round is canceled. We set this value to 300. This high value is not encouraged by the Hivemind framework, as it may cause optimizers to hang in case of network errors. However, because we have a controlled environment with low latency, setting this to a high value allows us to quickly determine issues with our setup and intervene by re-running the experiments.
- **grad_compression**; defines which class to use for gradient compression. We set this to `hivemind.NoCompression` for every run, as exploring the effects of compression for gradients is outside the focus of this thesis. Other works have focused on the effects of data sparsity and data parallelism [LTJ20].

5.3 Metrics comparison framework

In the next chapter, we will compare training and system metrics between baseline and Hivemind runs. However, they are not directly comparable.

Hivemind runs involve more than one machine per experiment, with each machine completing its task earlier or later than other peers that are in the same training network. We assume that an experiment ends when the last peer finishes processing the samples it has been assigned. Thus, for Hivemind runs we chose to use the maximum runtime amongst all peers to be used for comparison and analysis.

To compare baseline and Hivemind runs, we selected training accuracy as the metric of choice for three reasons. First, previous work on distributed training optimization tends to use accuracy to report their improvements, thus, using accuracy ourselves helps make better comparisons with other works. Second, accuracy is a function of the number of errors done across batches, while loss is a distance function that determines how big these errors are. This means that using accuracy is less subjective to which distance function we select, allowing for even broader comparisons for other works. Finally, training loss can be very unstable, potentially leading to very low values of loss at random, while accuracy is much more stable in that regard.

For training accuracy, we always select the average between the maximum training accuracy reached by the baseline re-runs, and the maximum accuracy reached by all peers for Hivemind runs. We chose the maximum for the Hivemind runs because the model being trained is essentially one. When saving the model for inference purposes,

the selection of which peer’s model to pick should lie on the model with the maximum loss achieved.

We use the average for system metrics such as bandwidth received and sent, CPU load and RAM usage for both baseline and Hivemind runs. This is because all nodes in our controlled Hivemind experiments behave more or less the same. In real-life scenarios such as training across the internet, where latency and peer behavior is unpredictable, this assumption would not be possible.

6 RESULTS

In this thesis, we are not looking to obtain the best possible combination of hyperparameters for training loss or model accuracy. Instead, we want to observe the effects on training with Hivemind when tuning common hyperparameters such as batch size and learning rate and Hivemind hyperparameters such as the TBS. In this thesis, we analyze the performance and limits of training using Hivemind rather than looking for the best model.

6.1 Baseline runs

We begin this chapter by showing the results that we have obtained with the baseline runs. As mentioned previously in chapter 4, all baseline experiments are executed on machines with the same configuration, and the total number of samples processed is always the same. Figure 6.1 shows the average runtimes for baseline runs in minutes. As we might have expected, most runs take more or less the same amount of time, as the total number of samples processed is the same for every run ¹.

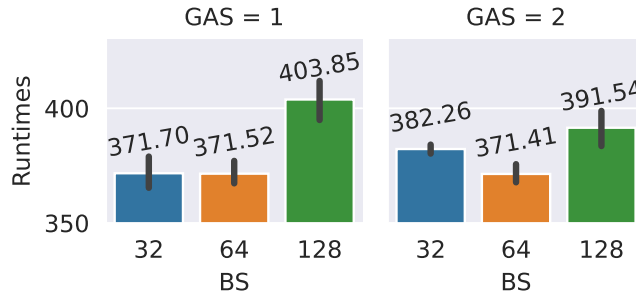


Figure 6.1: Average runtimes of baseline experiments in minutes. Runs are aggregated across LR, with the standard deviation amongst reruns as the black bar.

Baseline runs do not use distributed algorithms and all Hivemind features are switched off. However, Figure 6.3b shows that there is some network activity. On

¹BS=128 takes more time due to resource contention happening during the execution of the baseline runs.

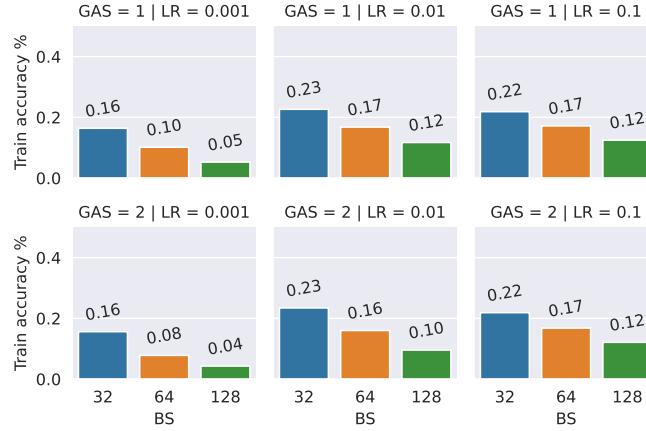


Figure 6.2: Maximum accuracy achieved by baseline runs, averaged across re-runs.

average, every machine receives a constant 1.5 MB/s of data on its network. This may be due to several factors, such as KVM management data, OpenNebula pings, and CEPH data being read.

In the Setup section, we also introduced our monitoring tool of choice *wandb*. Because this is an online monitoring tool, some data about our runs is periodically sent to the Weights and Biases server for storage and visualizations.

In Figure 6.3a, which shows the bandwidth used for send operations across all baseline runs, we can observe the bandwidth in MB/s used for each run. On average, this is roughly 0.02 MB/s on every run, a value that can be mostly attributed to *wandb* and other background monitoring operations such as OpenNebula.

In future sections, we will always account for these effects when performing comparisons with baseline runs.

Figure 6.4 shows the average times for data load, forward pass, backward pass and optimization step across batch sizes in baseline runs for both GAS=1 and GAS=2. As we might expect, the time it takes for a single step to complete is linearly dependent on the batch size. The learning rate (LR) does not affect the time it takes for each step to complete, so we aggregated the runs for each batch size. By contrast, the number of gradient accumulation steps (GAS) seems to shave off some time for every batch size. However, the total runtimes in Figure 6.1 do not seem to reflect this improvement. Because of this, throughout this chapter, we will keep showing GAS runs separately, as it still might affect some other aspects of training.

We further note that each step’s average time remains relatively unchanged throughout every experiment, given the same computational power, except for the data load

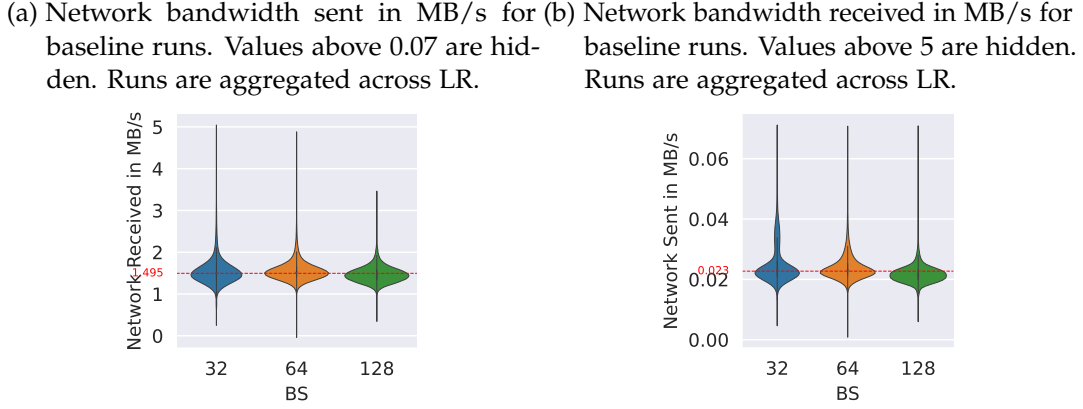


Figure 6.3: Network bandwidth sent and received in MB/s for baseline runs. Runs are aggregated across LR.

and optimizer steps ². The irregularity of the storage medium that we used for the experiment, CEPH, is to blame for the slight irregularities in the data load step. Regarding the optimizer step, its irregularities are due to two main factors: Hivemind settings and overcommitted nodes.

We will explore later in this chapter the effects of Hivemind settings on the optimizer step. Overcommitted nodes are a consequence of the cloud environment where the machines that perform our experiments are set up. Because we have limited resources in our cluster, sometimes other researchers may need to overcommit the same node vCPUs to perform their experiments. This causes several issues when training in a distributed setting with Hivemind, such as nodes not responding for long periods of time, sometimes even minutes. In such cases, two things can happen:

- if the non-responding node or nodes were not participating in an averaging round, other participating nodes will wait for 10 seconds, and then start an averaging round without other nodes;
- if the node was actively participating in an averaging round, nodes will wait for the node to come back for 300 seconds or five minutes.

Future efforts to replicate the results presented in this thesis may wish to pin their resources to prevent or reduce these issues from happening.

²We will not show anymore the times of every step besides the optimizer step, as they remain generally constant.

In Figure 6.4 we can also notice the big impact that data loading has on every step. Almost 1/2 of the total time for each step consists in waiting for the data to load. As we increase the number of cores per peer, CPU utilization decreases, as the CPU is idle during I/O wait times and normal operations such as forward and backward pass take less time. This is a bottleneck that can easily be tackled through several means, such as having a faster storage backend or if that is not available, faster data loader frameworks and algorithms [Ise+22; Lec+22]. Future work may make use of local, faster storage backed by SSD to achieve faster data load speeds, helping us rule out the effects of data loading on training with Hivemind.

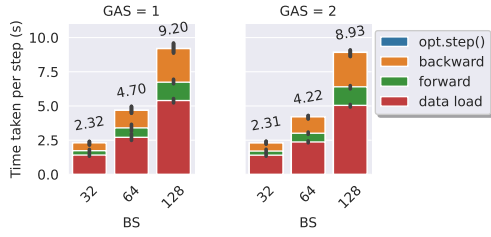


Figure 6.4: Average times of step data load (red), forward pass (green), backward pass (orange) and optimization step (blue) baseline experiments in seconds. Runs are further aggregated across LR and the standard error amongst runs is shown with black bars.

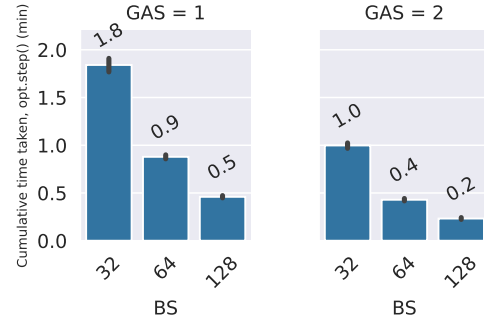


Figure 6.5: Cumulative time taken by the `opt.step()` for every batch size, in minutes. Runs are further aggregated across LR and the standard error amongst runs is shown with black bars.

Finally, we zoom in on the effect of GAS for baseline runs on the optimizer step times in Figure 6.5. The graph shows the total amount of time spent for each run to perform `opt.step()`, grouped by LR. As we might expect from Algorithm 2, doubling GAS led to half the time spent on the optimizer step, as it is called exactly half of the time. Furthermore, as we increase the batch size, we also reduce the amount of time spent performing the optimization step. Because backpropagation scales with the number of outputs, performing the optimization step does not scale up with the increased input size. In the next sections, we will further analyze the effects of using GAS together with other Hivemind settings.

6.2 Focus on effects of batch size, learning rate and target Batch Size

Batch size and learning rate are some of the most fundamental hyperparameters to tune when training a neural network to obtain good training results. Tuning the learning rate should not impact training performance directly, but it can help to better understand how to tune it for different settings combinations while using Hivemind. As specified previously in chapter 4, the reference optimizer algorithm is the stochastic gradient descent (SGD), which is wrapped around the `hivemind.Optimizer` class.

The batch size determines how many samples are being processed in a training loop. In Hivemind, this has the consequence of reaching the TBS in fewer steps, but not necessarily in less time.

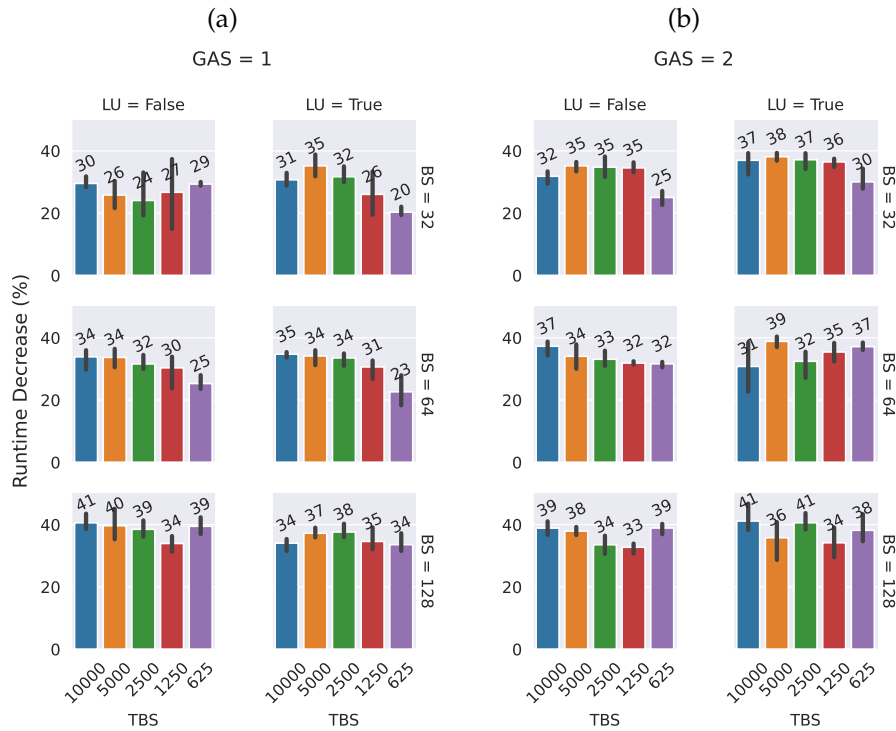


Figure 6.6: Runtime decrease in percent for Hivemind runs with 2 peers and 8vCPUs relative to the baseline runs. Higher is better. Runs are aggregated across LR and the standard error amongst runs is shown with black bars.

Figure 6.6 shows the runtimes for Hivemind experiments with 2 peers and 8vCPUs per peer compared to the baseline runs. Every run shows a substantial decrease in

runtime, with $BS = 32$ having an average decrease of circa 20%, $BS = 64$ of circa 30% and close to 40% for $BS = 128$. But can we just expect such a high increase in performance for free when turning on Hivemind? There are two important factors to take into consideration before making a such claim.

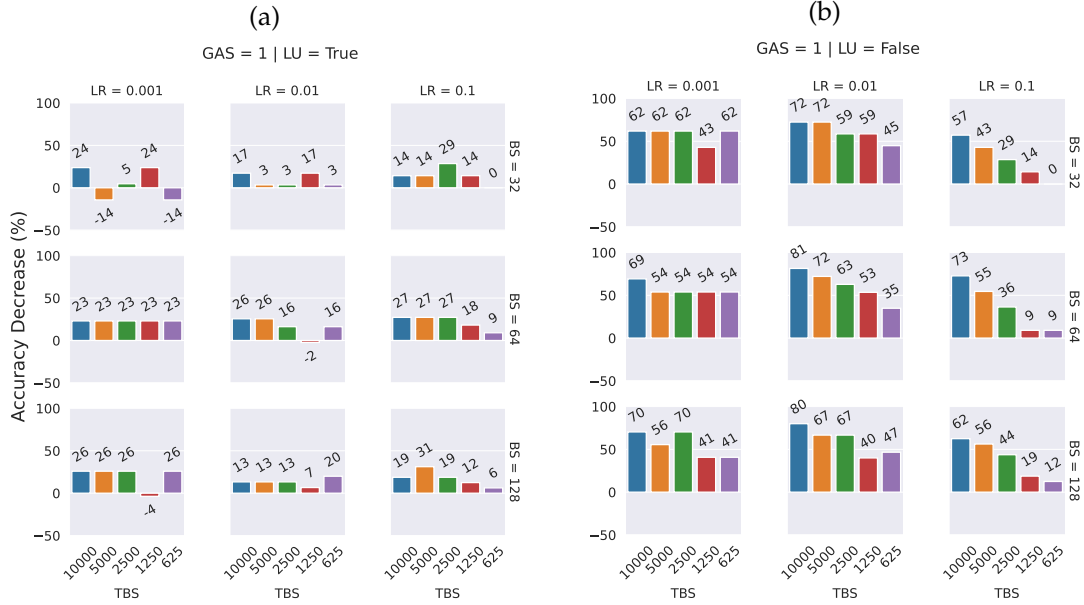


Figure 6.7: GAS=1, accuracy decrease in percent for Hivemind runs with 2 peers and 8vCPUs relative to the baseline runs. Higher is worse.

1. Data loading in the baseline runs takes 1/3 of the total time per step as shown in Figure 6.4. Parallelizing data loading indeed speeds up the overall runtime for each run. With further experimentation that is outside the scope of this thesis, it might be possible to reduce the data loading step with local parallelization techniques and faster storage. Reducing the data loading step might help rule out the possibility that we only see runtime improvements because of the effects of loading more data in parallel.
2. The results in Figure 6.7 and Figure 6.8 shows the hidden impact on accuracy of using Hivemind. Nearly all experiments are not able to reach the maximum accuracy set by the respective baseline runs. Some experiments [YGG17] have shown that large batch training can lead to divergence, and it is possible to reach the same model accuracy just by training longer. Others [Kes+16] argue

that longer training with larger batch sizes might lead to overall worse generalization capabilities for the model. Proving the effects on accuracy and model generalization is beyond the scope of this thesis.

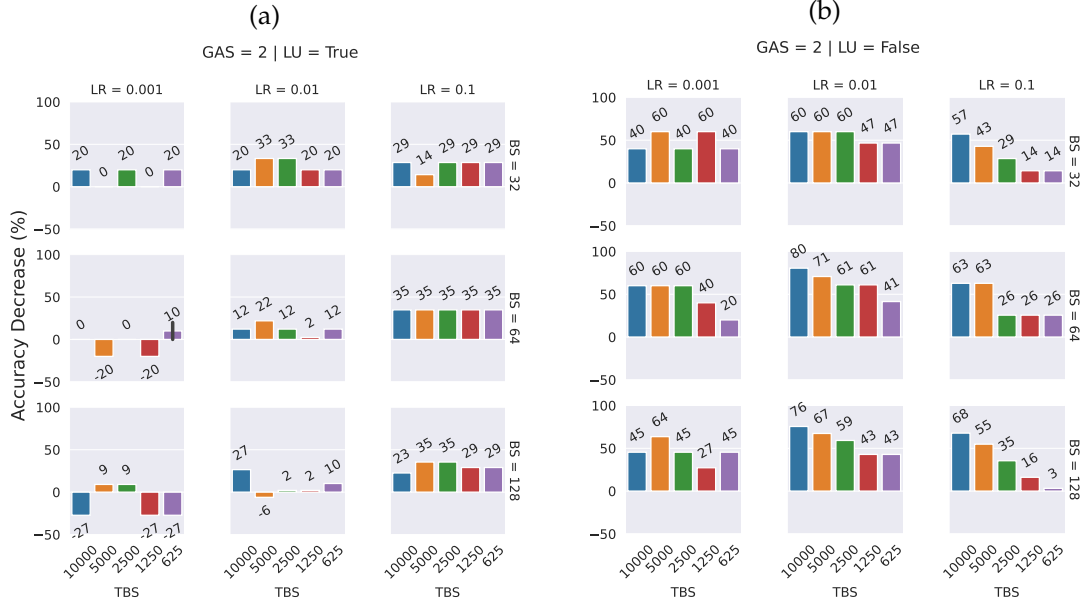


Figure 6.8: GAS=2, accuracy decrease in percent for Hivemind runs with 2 peers and 8vCPUs relative to the baseline runs. Higher is worse.

Depending on the optimizer used for training a neural network model, the number of parameters can become huge. When performing an optimizer state averaging state, sending a high amount of parameters can lead to high communication overhead, and thus, reduced performance [HHS17; LTJ20; Dea+12a; Sha+18]. However, this effect is almost non-existent for small neural networks such as ResNet18 [Zha+20].

Figure 6.9 and Figure 6.10 show that the bandwidth utilization is very low for a local network such as that of the setup of our experiment. Consequently, none of our Hivemind experiments ever reached network bandwidth saturation for both receive and send operations. Furthermore, the Hivemind settings of our experiments do not allow overlapping training operations with averaging operations, which are all executed during the `opt.step()` call. Gradients are thus sent and received in a single step rather than in the background, which in our experiments did not lead to any discernible bottleneck.

Taking a look back at Figure 2.5 and Figure 2.4, we expect that as we increase TBS,

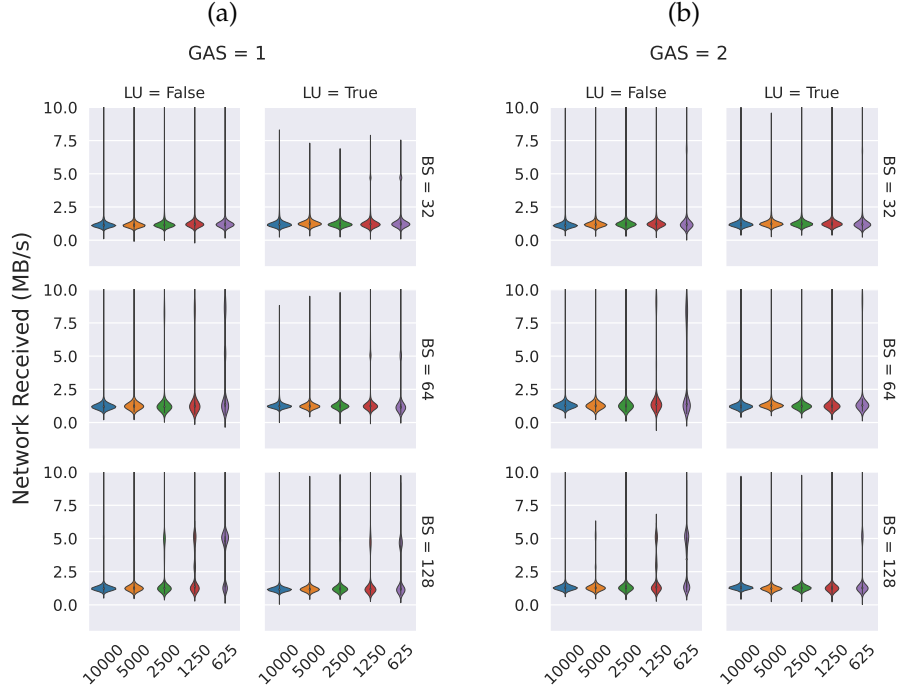


Figure 6.9: Network received for Hivemind runs with 2 peers and 8vCPUs. Values ≥ 10 MB/s are hidden and runs are aggregated across LR.

we should see the time spent on `opt.step()` increase. This is because nodes perform more steps overall, and thus spend more time looking for peers to perform averaging with. Furthermore, we should see that as we increase the batch size, we also spend less time performing the optimization step, as we do fewer calls to `opt.step()` in total. Figure 6.11 shows the cumulative time taken for the optimization step in every run, aggregated per LR. Generally, we see that our expectations are confirmed across all runs, with some exceptions ³.

Considerations of training with Hivemind for the TBS, BS and LR hyperparameters:

- With the same amount of computational power overall, training with Hivemind might need more time to reach a target accuracy compared to the baseline runs.
- Having access to less powerful hardware still allows training peers to be helpful, at the cost of training for longer.

³The imperfect environment that our experiments are performed on allows node overcommitting, causing some runs to show increased waiting times.

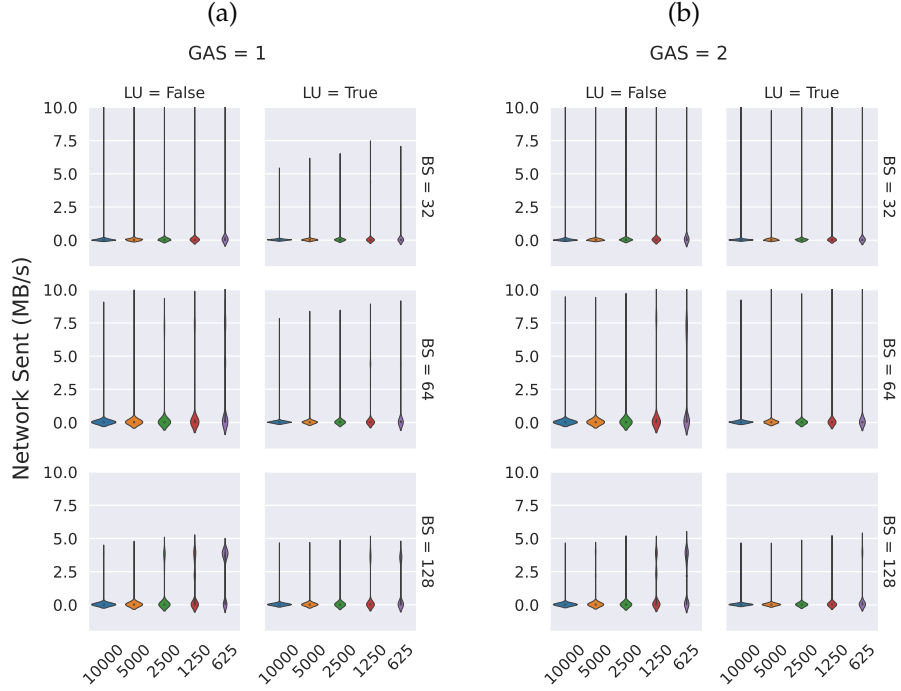


Figure 6.10: Network sent for Hivemind runs with 2 peers and 8vCPUs. Values ≥ 10 MB/s are hidden and runs are aggregated across LR.

- Averaging more frequently, thus increasing TBS can help to reduce the accuracy gap with the baseline runs.
- Increasing TBS does not make up for a bad selection of optimization hyperparameters such as the batch size and learning rate.
- Trying to get closer accuracy by increasing TBS may lead to fewer benefits in terms of total runtime reduction, as we spend increasingly more time waiting for averaging peers and averaging operations.

6.3 Focus on effects of gradient accumulation

Gradient accumulation allows the simulation of bigger batches within a single node by accumulating gradients every time the backpropagation step is performed. After GAS steps, the optimizer step is performed and the gradients are finally applied to the trained model. We have previously shown that as we reduce the number of calls to the

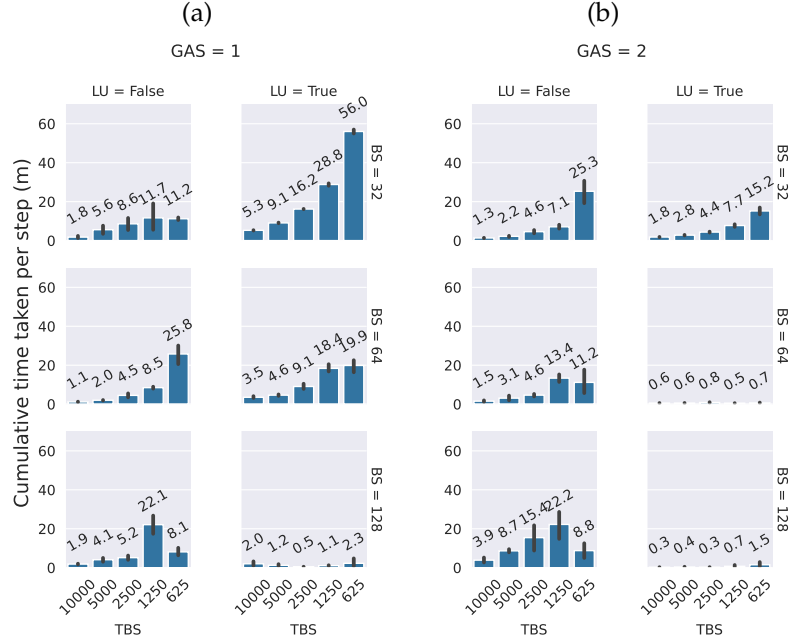


Figure 6.11: Cumulative time taken by the `opt.step()` for Hivemind experiments with 2 peers and 8vCPUs in minutes. Runs are further aggregated across LR and the standard error amongst runs is shown with black bars (continues).

optimizer, we also see a reduction in overall time spent in this step. Increasing GAS to two should also reduce this, as we perform one `opt.step()` call every two steps. This is confirmed by looking at Figure 6.11, where we see that compared to GAS=1, GAS=2 runs spend much less time on average for optimizer operations.

Regarding accuracy, we notice that for baseline runs increasing GAS can help increase accuracy by some points relative to the baseline runs. In Figure 6.7 and Figure 6.8 we can see the accuracy decrease with respect to the baseline runs in four different configurations:

- GAS=1, LU=True;
- GAS=1, LU=False;
- GAS=2, LU=True;
- GAS=2, LU=False;

With both LU=True and LU=False, we can notice a better accuracy with GAS=2 by 5-10% compared to GAS=1 for experiments with high LR. Thus, as LR increases, the

gap between GAS=1 and GAS=2 closes, with the gap getting even closer for smaller TBS values. However, this is not consistent with all runs, and we would suggest re-running some experiments to confirm this point. It remains an open question whether increasing GAS to higher values than 2 will lead to experiments with LU=False eventually becoming better than the baseline runs.

Finally, we notice that the impact on network utilization using our experiment combination of configurations is minimal. For scenarios with more traffic, high values of GAS may help reduce the number of times that the Hivemind optimizer is called, reducing step time.

Evaluating the effects of using gradient accumulation and averaging, we can say the following when training ResNet18 on Imagenet with Hivemind:

- the smaller the TBS, the less the difference between GAS=1 and GAS=2 matters. It remains an open question whether this statement holds for higher values of GAS.
- for high values of LR, GAS does not seem to affect training as much as for low values of LR.

6.4 Focus on effects of local updates

By default, the Hivemind Optimizer wraps around a Pytorch optimizer, taking control of underlying actions such as the application of gradients to the underlying model. When local updates (LU) are enabled, gradients are applied directly to the model at each call of the Hivemind Optimizer. When LU are disabled, the gradients are only applied to a model after the gradient averager and state averager have finished.

Taking a look at Figure 6.6, we can notice that the runtime difference between enabling or disabling local updates is minimal and perhaps not relevant. As we can notice by the very low bandwidth usage in both Figure 6.9 and Figure 6.10, LU also has little effect on networking for our setup. This may be due to several factors, such as the relatively small size of the model and the optimizer

In Figure 6.7 and Figure 6.8 the difference between the two modes in terms of accuracy decrease compared to the baseline is quite noticeable. Disabling local updates consistently leads to worse performance compared to the baseline experiments with the highest accuracy. However, for low accuracy increase, the results are not entirely relevant. The final accuracy is still too low to be considered a good training result compared to the baseline experiments.

For both GAS=1 and GAS=2, we can observe that the penalty for disabling local updates with large values of target batch size is very big. As we increase the TBS, this penalty goes up even further, sometimes more than 50% compared to enabling local

updates. As previously stated, for small runs such as the ones presented in this thesis, the impact of using local updates is virtually negligible, and thus can be preferred. It is currently an open question if this will hold for larger models and a higher number of peers.

Increasing GAS also yields interesting results for LU=True. Because GAS=2 prevents updating the underlying model for one step, we can see the negative effects of enabling local updates, which rely on applying the gradients at every step to perform averaging between all peers. We can see this effect especially for larger LR values. This can have serious implications when simulating bigger batch sizes, as this is usually done by accumulating gradients and thus increasing GAS.

In short, this is what we learned from the effects of local updates:

- Enabling local updates seems to work best at virtually no cost to overall performance using the setup presented in this thesis.
- Disabling local updates is more unforgiving in terms of the accuracy decrease, with additional penalties as the target batch size increases and thus the waiting time between averaging rounds. As long as peers can communicate as often as possible however this does not seem to be an issue.
- Increasing GAS with local updates enabled may cause worse performance in terms of accuracy, taking into account baseline runs with good performance.
- On the contrary, with disabled local updates, GAS=2 leads to overall better accuracy compared to GAS=1, but it is still bad with respect to baseline runs.

6.5 Focus on effects of the number of peers and vCPUs per peer

Institutions and companies may have more than two machines at their disposal to perform distributed training. So far, we have explored the effects on Hivemind of specific settings such as TBS, BS LR, GAS and LU. Adding more nodes to a distributed training setting can lead to bottlenecks, especially when using a client-server approach [AJR21; MCA19]. In this section, we answer the following research question: what are the effects of scaling up the number of machines when using Hivemind?

The frequency at which peers average their model state is directly proportional to the number of peers, the throughput per second of each peer and the TBS. In turn, the throughput per second is affected by several factors such as the BS, computational power of the node and wait times for I/O operations.

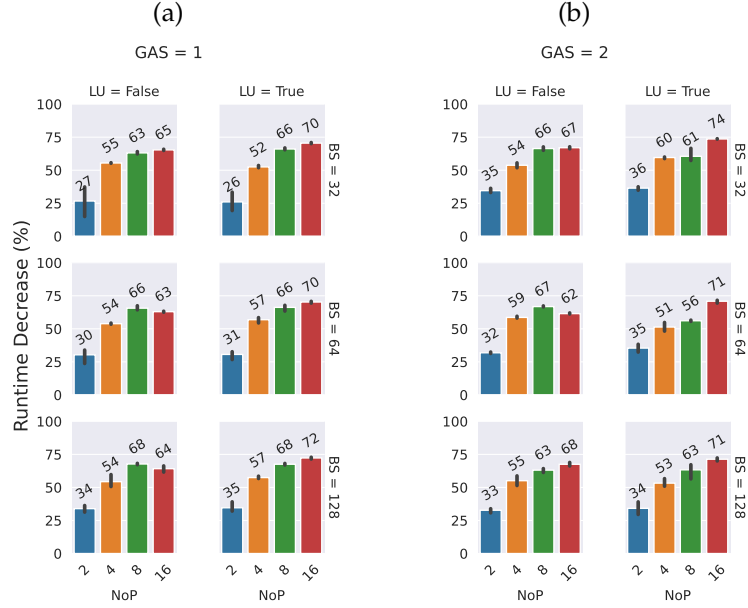


Figure 6.12: Runtime decrease in percent for Hivemind runs with 2, 4, 8, 16 peers and 8, 4, 2, 1 vCPUs respectively relative to baseline runs. Higher is better. Runs are aggregated across LR and the standard error amongst runs is shown with black bars.

It might be difficult to isolate the effects of introducing more nodes from scaling the target batch size. Thus, we decided to fix the target batch size to 1250 for this set of experiments and alter TBS, BS, LR, GAS and LU.

As we might expect, Figure 6.12 shows that increasing the number of peers dramatically decreases runtime. The highest jump in runtime performance is between using one single peer (Hivemind disabled) and using two peers (Hivemind enabled). Introducing four peers also cuts down runtime by around 50% compared to using two peers across all experiments. However, this effect does not appear to be linear. The benefits of including more peers only increase by 10-15% for eight peers and 4-6% for sixteen peers. If we take into consideration the decreased accuracy performance, there seems to be a sweet spot in terms of reducing the total runtime and an acceptable reduction in accuracy performance. Using four peers seems to be the optimal number of peers when training with Hivemind on our configuration to obtain the maximum reduction of runtime without having a significant hit in terms of accuracy. It remains an open question whether training these runs for longer would yield the same accuracy as the baseline runs but in less time overall. Further experimentation may also show

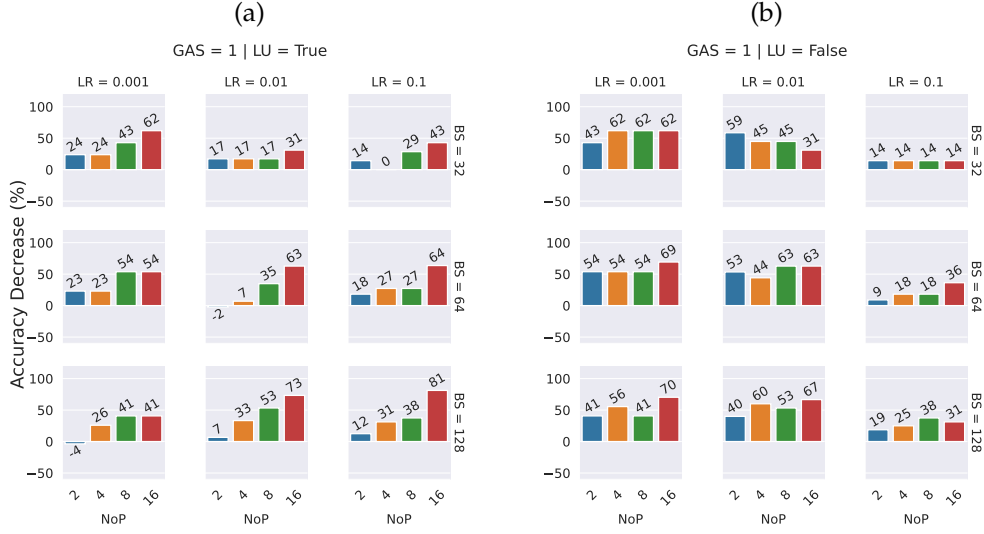


Figure 6.13: GAS = 1, accuracy decrease in percent for Hivemind runs with 2, 4, 8, 16 peers and 8, 4, 2, 1 vCPUs respectively relative to baseline runs. Higher is worse.

that increasing the TBS, and thus reducing the averaging frequency amongst peers, can be beneficial in runs where TBS is quickly reached.

Figure 6.13 shows that GAS and LU settings seem to generally have a similar effect compared to Hivemind runs with 2 peers and 8vCPUs presented in section 6.2. The graph also shows us a decrease in performance as we increase the number of peers, especially for experiments that have reached a higher accuracy. In general, we noticed that compared to baseline experiments with bad performance, the accuracy does not change too much when using Hivemind.

Figure 6.15 shows the cumulative time in minutes taken by the optimization step for the Hivemind experiments changing NoP. We can notice little changes when increasing from GAS=1 to GAS=2 when local updates are disabled, with a slight increase in processing time as we increase the NoP. This is to be expected, as the more peers are introduced, the more often peers can perform averaging. However, this effect is dampened by the simultaneous reduction in the processing speed of every node.

When local updates are enabled, the difference between GAS=1 and GAS=2 are instead much more noticeable, with GAS=2 drastically reducing the time spent on the optimization step. This may be because peers call less frequently `opt.step()`, they perform fewer averaging rounds overall. As the number of peers increases, we also see a reduction in time spent. This is also due to the reduced number of maximum steps

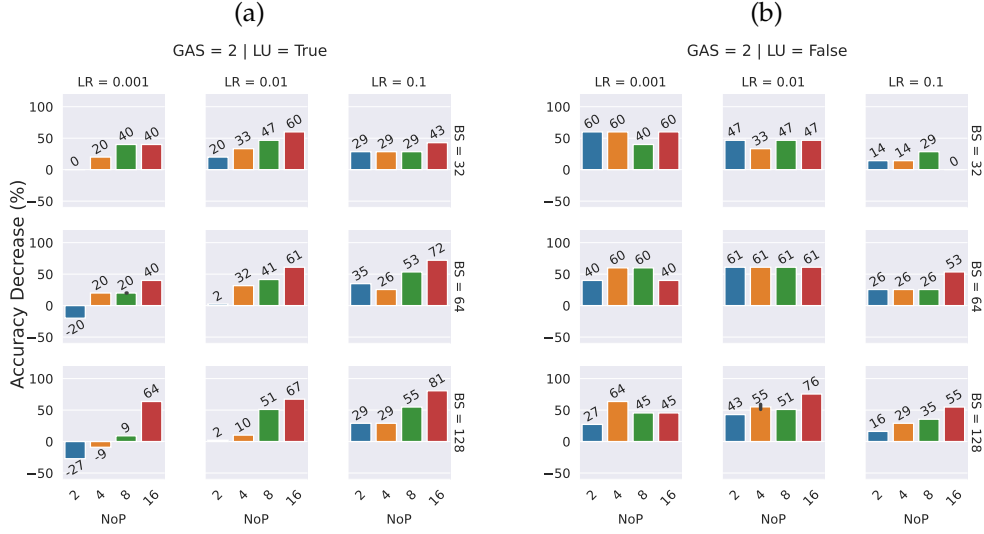


Figure 6.14: GAS = 2, accuracy decrease in percent for Hivemind runs with 2, 4, 8, 16 peers and 8, 4, 2, 1 vCPUs respectively relative to baseline runs. Higher is worse.

called, which becomes half again if we increase GAS.

The network bandwidth utilization for different peer configurations is shown in Figure 6.16 and Figure 6.17, and yield interesting results. As we increase the number of peers in a training session, peers communicate more often, which can also be seen as these "bulbs" in the violin plots. This is unsurprising, for two reasons: first, the time to reach the fixed TBS of 1250 gets shorter as we add more peers, thus, the frequency at which peers communicate increases with the number of peers; second, with more peers to average with, there is more data to exchange in terms of pings, synchronization messages and such. We can see that with sixteen peers, the sent bandwidth utilization is almost exclusively around 5MB/s. Nevertheless, even with sixteen peers, we did not see any significant CPU bottleneck caused by high network communication.

Finally, we make different observations for GAS and LU values as we presented in section 6.4 and section 6.3. Enabling LU for a higher number of peers seems to be very penalizing, especially with NoP=16. Disabling LU instead yields more consistent accuracies in every experiment but seems to perform best for large values of LR. Increasing GAS appears to worsen the situation when paired with LU=True, except for very low values of LR. On the other hand, increasing GAS to 2 while disabling local updates seems to be a bit better, but not as consistently as decreasing TBS in section 6.2.

Summarizing the findings, we can say the following for our setup:

- Increasing the number of peers while maintaining the same computational power can reduce the total runtime by at least 30%.
- However runtime reduction is not linear compared to the number of peers. The effects of reducing the data load times by using faster storage are still an open question.
- With local updates enabled, increasing the number of peers seems to have a worse effect on training accuracy. The effects of other values of TBS for a different number of peers is still an open question.
- Introducing more peers leads to more bandwidth usage as each peer exchanges more data with other averaging partners. This effect can become much larger for larger models and a much larger number of nodes.
- At the same time, increasing the number of peers reduces the amount of time spent averaging given a fixed sample budget.

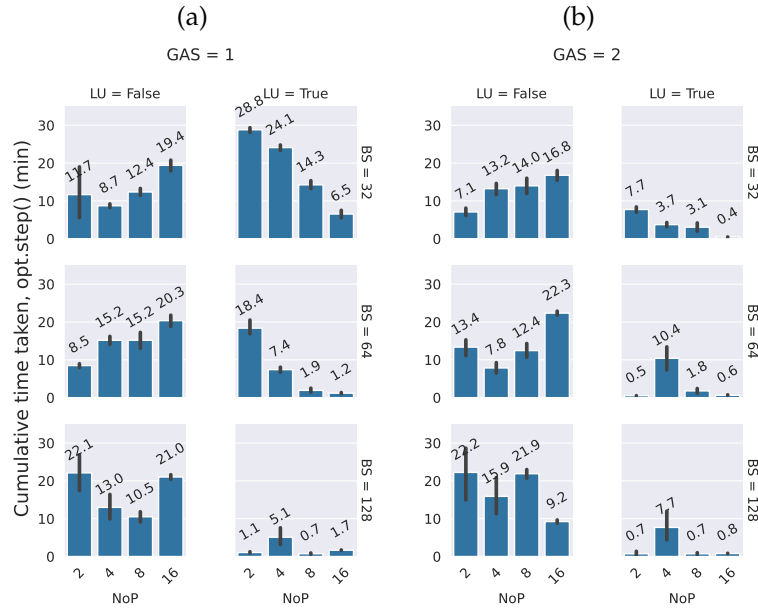


Figure 6.15: Cumulative time taken by the `opt.step()` for Hivemind runs with 2, 4, 8, 16 peers and 8, 4, 2, 1 vCPUs respectively in minutes. Runs are further aggregated across LR.

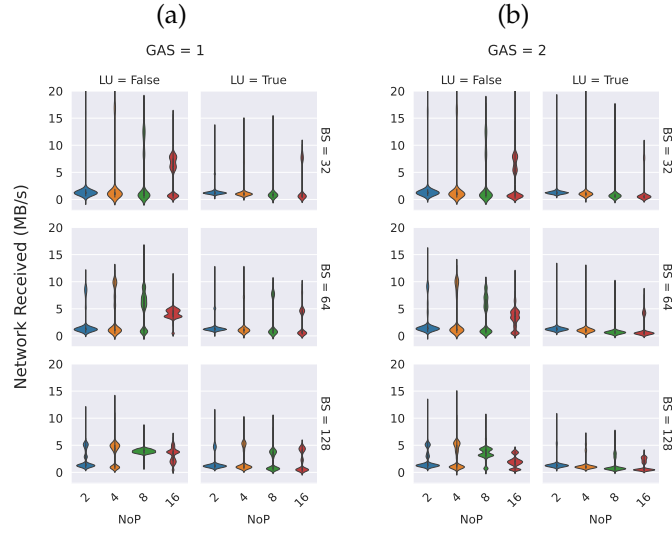


Figure 6.16: Network received for Hivemind runs with 2, 4, 8, 16 peers and 8, 4, 2, 1 vCPUs respectively. Values ≥ 20 MB/s are hidden and runs are aggregated across LR.

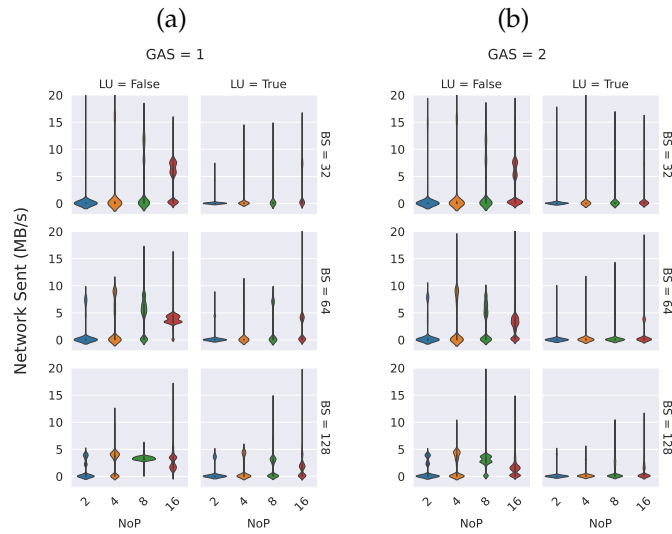


Figure 6.17: Network sent for Hivemind runs with 2, 4, 8, 16 peers and 8, 4, 2, 1 vCPUs respectively. Values ≥ 20 MB/s are hidden and runs are aggregated across LR.

7 FUTURE WORK

Hivemind is a great tool enabling collaborative training for neural networks. However, studies targeting this area are limited, thus limiting the possibilities for comparison between other frameworks and approaches. It may be possible to build collaborative training frameworks on top of the basic Hivemind concepts which are tuned specifically for fast connections. This could allow stable collaborative training amongst entities with idle resources. Entities that do not wish to keep training may be able to just drop out of the peer network without a huge impact on overall training.

Other applications for Hivemind can be secure, distributed training. Some companies may be reluctant to share their data but may be willing to use their own resources to collaboratively train a model with other entities. Hivemind may help by allowing companies with sensitive data to join a collaborative network without having to share their data. Future work may analyze the impact of using different datasets on training with Hivemind, and potential security issues that may arise with gradient sharing, authentication and byzantine scenarios [Gor+21].

Our approach in analyzing Hivemind bottlenecks was primarily focused on a small set of hyperparameters, both for training and for Hivemind. Furthermore, the model that we chose for our experiments, ResNet18, is very small compared to other works. Future experiments on Hivemind should focus on reaching a network bottleneck without any compression, and then analyze the effects of using different gradient compression strategies. This can help us understand better the effects of introducing additional time for computation versus time used for communication.

Our cluster uses CEPH as the distributed data store, which has been great for ease of use and bootstrapping our experiments. However, we encountered many limitations along the way, such as sudden spikes in data load times caused by other colleagues performing read/write operations on the cluster. Because of this, many experiments had to be repeated to avoid exaggerated skews in data load times. For better and more reliable results, future work should stick to local I/O operations to rule out possible external pollution of experiment results. Newer data loading algorithms such as FFCV [Lec+22] can help reduce data loading times even more, further which may have a big impact when training with lower-end devices.

We have run Hivemind using low-tier devices with up to 8vCPUs using 8GB of RAM, which are more than good enough for training ResNet18. However, current state-of-

the-art demands training deeper and bigger models such as ResNet101 and VGGNet16 [SZ14]. Running Hivemind experiments on beefier devices such as GPUs and TPUs to further reduce the time of synchronous train operations such as forward and backward pass could yield interesting results. This would help us get a better understanding of what Hivemind can do in the best-case scenarios and possible bottlenecks.

Finally, in this thesis we focused on changing several training hyperparameters, skipping the selection and the impact of optimizers and schedulers. Past work suggested pairing large batch training with specialized optimizer functions such as LARS for convolution-based networks [YGG17; Kes+16] and LAMB for language-based networks [You+19]. Testing Hivemind by simulating larger batches has been previously done by the authors of Hivemind [Dis+21], but it was only limited to SwAV [Car+20]. Future work may try to perform large batch training on Hivemind by exploring several combinations of hyperparameters with the scope of achieving comparable results with the current state-of-art.

8 CONCLUSIONS

In this work, we analyze Hivemind, a framework for deep learning volunteer computing over the internet. The analysis focuses on the effects of common training hyperparameters such as batch size and training rate, as well as Hivemind hyperparameters such as training batch size and the number of peers. We show that it can successfully be used to collaboratively train smaller deep learning networks such as ResNet18 using the Imagenet dataset, with a few caveats.

Our investigation on training hyperparameters and Hivemind settings reveals three major points for the setup that we selected: first, we found that training with the Hivemind local updates setting turned on is beneficial for our particular setup, at virtually no cost; second, using gradient accumulation can lead to worse loss when enabling local updates and better loss when disabling it; third, network bottlenecks for such a low number of parameters are not an issue in any scenario.

Finally, we show the effects of training Hivemind on more than two devices while maintaining the same sample and computational power budget. There is a sweet spot in terms of runtime benefits and loss when adding more nodes. After adding enough peers to a training network, the reduction of runtime does not increase enough to justify loss penalties.

List of Figures

1.1	GPU VRAM over the past 4 years. The growth is mostly linear, doubling	2
1.2	Model size over the past 4 years, in logarithmic scale: ELMo [Pet+18], BERT [Dev+18], GPT-2 [Rad+19], Megatron-LM [Sho+19], T-5 [Raf+19], Turing-NLG [Mic20], GPT-3 [Bro+20], Megatron-Turing-NLG [Smi+22]	3
2.1	An example of a neural network, with input layers (green nodes), hidden layers (blue nodes), and output layer (red node).	7
2.2	Nodes in a Peer-to-Peer network exchanging data directly with one another. Every node has its own internal DHT which is kept in sync with other peers.	14
2.3	State averaging (left) and gradient averaging (right) in Hivemind.	15
2.4	Diagram of Hivemind training with local updates enabled.	17
2.5	Diagram of Hivemind training with local updates disabled.	18
6.1	Average runtimes of baseline experiments in minutes. Runs are aggregated across LR, with the standard deviation amongst reruns as the black bar.	31
6.2	Maximum accuracy achieved by baseline runs, averaged across re-runs.	32
6.3	Network bandwidth sent and received in MB/s for baseline runs. Runs are aggregated across LR.	33
6.4	Average times of step data load (red), forward pass (green), backward pass (orange) and optimization step (blue) baseline experiments in seconds. Runs are further aggregated across LR and the standard error amongst runs is shown with black bars.	34
6.5	Cumulative time taken by the <code>opt.step()</code> for every batch size, in minutes. Runs are further aggregated across LR and the standard error amongst runs is shown with black bars.	34
6.6	Runtime decrease in percent for Hivemind runs with 2 peers and 8vCPUs relative to the baseline runs. Higher is better. Runs are aggregated across LR and the standard error amongst runs is shown with black bars.	35
6.7	GAS=1, accuracy decrease in percent for Hivemind runs with 2 peers and 8vCPUs relative to the baseline runs. Higher is worse.	36

6.8	GAS=2, accuracy decrease in percent for Hivemind runs with 2 peers and 8vCPUs relative to the baseline runs. Higher is worse.	37
6.9	Network received for Hivemind runs with 2 peers and 8vCPUs. Values ≥ 10 MB/s are hidden and runs are aggregated across LR.	38
6.10	Network sent for Hivemind runs with 2 peers and 8vCPUs. Values ≥ 10 MB/s are hidden and runs are aggregated across LR.	39
6.11	Cumulative time taken by the <code>opt.step()</code> for Hivemind experiments with 2 peers and 8vCPUs in minutes. Runs are further aggregated across LR and the standard error amongst runs is shown with black bars (continues).	40
6.12	Runtime decrease in percent for Hivemind runs with 2, 4, 8, 16 peers and 8, 4, 2, 1 vCPUs respectively relative to baseline runs. Higher is better. Runs are aggregated across LR and the standard error amongst runs is shown with black bars.	43
6.13	GAS = 1, accuracy decrease in percent for Hivemind runs with 2, 4, 8, 16 peers and 8, 4, 2, 1 vCPUs respectively relative to baseline runs. Higher is worse.	44
6.14	GAS = 2, accuracy decrease in percent for Hivemind runs with 2, 4, 8, 16 peers and 8, 4, 2, 1 vCPUs respectively relative to baseline runs. Higher is worse.	45
6.15	Cumulative time taken by the <code>opt.step()</code> for Hivemind runs with 2, 4, 8, 16 peers and 8, 4, 2, 1 vCPUs respectively in minutes. Runs are further aggregated across LR.	46
6.16	Network received for Hivemind runs with 2, 4, 8, 16 peers and 8, 4, 2, 1 vCPUs respectively. Values ≥ 20 MB/s are hidden and runs are aggregated across LR.	47
6.17	Network sent for Hivemind runs with 2, 4, 8, 16 peers and 8, 4, 2, 1 vCPUs respectively. Values ≥ 20 MB/s are hidden and runs are aggregated across LR.	47

List of Tables

4.1	List of key host metrics logged using psutil.	22
4.2	List of key host metrics logged using psutil.	24
5.1	List of baseline experiments and hyperparameters	27
5.2	List of Hivemind experiments and hyperparameters. Every experiment has been executed once, and every time with at least two peers.	28

Bibliography

- [AJR21] M. Atre, B. Jha, and A. Rao. “Distributed Deep Learning Using Volunteer Computing-Like Paradigm.” In: *2021 IEEE International Parallel and Distributed Processing Symposium Workshops (IPDPSW)*. IEEE, June 2021. doi: 10.1109/ipdpsw52791.2021.00144.
- [Beb+09] A. L. Beberg, D. L. Ensign, G. Jayachandran, S. Khaliq, and V. S. Pande. “Folding@home: Lessons from Eight Years of Volunteer Distributed Computing.” In: *Proceedings of the 2009 IEEE International Symposium on Parallel and Distributed Processing*. IPDPS ’09. USA: IEEE Computer Society, 2009, pp. 1–8. ISBN: 9781424437511. doi: 10.1109/IPDPS.2009.5160922.
- [Bla+20] D. Blalock, J. J. G. Ortiz, J. Frankle, and J. Gutttag. *What is the State of Neural Network Pruning?* 2020. doi: 10.48550/ARXIV.2003.03033.
- [Bro+20] T. B. Brown, B. Mann, N. Ryder, M. Subbiah, J. Kaplan, P. Dhariwal, A. Neelakantan, P. Shyam, G. Sastry, A. Askell, S. Agarwal, A. Herbert-Voss, G. Krueger, T. Henighan, R. Child, A. Ramesh, D. M. Ziegler, J. Wu, C. Winter, C. Hesse, M. Chen, E. Sigler, M. Litwin, S. Gray, B. Chess, J. Clark, C. Berner, S. McCandlish, A. Radford, I. Sutskever, and D. Amodei. “Language Models are Few-Shot Learners.” In: *CoRR abs/2005.14165* (2020). arXiv: 2005.14165.
- [Car+20] M. Caron, I. Misra, J. Mairal, P. Goyal, P. Bojanowski, and A. Joulin. “Unsupervised Learning of Visual Features by Contrasting Cluster Assignments.” In: *CoRR abs/2006.09882* (2020). arXiv: 2006.09882.
- [Dea+12a] J. Dean, G. S. Corrado, R. Monga, K. Chen, M. Devin, Q. V. Le, M. Z. Mao, M. Ranzato, A. Senior, P. Tucker, K. Yang, and A. Y. Ng. “Large Scale Distributed Deep Networks.” In: *Proceedings of the 25th International Conference on Neural Information Processing Systems - Volume 1*. NIPS’12. Lake Tahoe, Nevada: Curran Associates Inc., 2012, pp. 1223–1231.
- [Dea+12b] J. Dean, G. S. Corrado, R. Monga, K. Chen, M. Devin, Q. V. Le, M. Z. Mao, M. Ranzato, A. Senior, P. Tucker, K. Yang, and A. Y. Ng. “Large Scale Distributed Deep Networks.” In: *NIPS*. 2012.

- [Den+09] J. Deng, W. Dong, R. Socher, L.-J. Li, K. Li, and L. Fei-Fei. "ImageNet: A large-scale hierarchical image database." In: *2009 IEEE Conference on Computer Vision and Pattern Recognition*. 2009, pp. 248–255. DOI: 10.1109/CVPR.2009.5206848.
- [Dev+18] J. Devlin, M.-W. Chang, K. Lee, and K. Toutanova. "BERT: Pre-training of Deep Bidirectional Transformers for Language Understanding." In: *CoRR abs/1810.04805* (2018). arXiv: 1810.04805.
- [Dis+21] M. Diskin, A. Bukhtiyarov, M. Ryabinin, L. Saulnier, Q. Lhoest, A. Sinitsin, D. Popov, D. V. Pyrkin, M. Kashirin, A. Borzunov, A. V. del Moral, D. Mazur, I. Kobelev, Y. Jernite, T. Wolf, and G. Pekhimenko. "Distributed Deep Learning in Open Collaborations." In: *CoRR abs/2106.10207* (2021). arXiv: 2106.10207.
- [Gor+21] E. Gorbunov, A. Borzunov, M. Diskin, and M. Ryabinin. "Secure Distributed Training at Scale." In: *CoRR abs/2106.11257* (2021). arXiv: 2106.11257.
- [Goy+17] P. Goyal, P. Dollár, R. B. Girshick, P. Noordhuis, L. Wesolowski, A. Kyrola, A. Tulloch, Y. Jia, and K. He. "Accurate, Large Minibatch SGD: Training ImageNet in 1 Hour." In: *CoRR abs/1706.02677* (2017). arXiv: 1706.02677.
- [He+15] K. He, X. Zhang, S. Ren, and J. Sun. "Deep Residual Learning for Image Recognition." In: *CoRR abs/1512.03385* (2015). arXiv: 1512.03385.
- [HHS17] E. Hoffer, I. Hubara, and D. Soudry. "Train longer, generalize better: closing the generalization gap in large batch training of neural networks." In: (2017). DOI: 10.48550/ARXIV.1705.08741.
- [HMD15] S. Han, H. Mao, and W. J. Dally. *Deep Compression: Compressing Deep Neural Networks with Pruning, Trained Quantization and Huffman Coding*. 2015. DOI: 10.48550/ARXIV.1510.00149.
- [Hua+18] Y. Huang, Y. Cheng, D. Chen, H. Lee, J. Ngiam, Q. V. Le, and Z. Chen. "GPipe: Efficient Training of Giant Neural Networks using Pipeline Parallelism." In: *CoRR abs/1811.06965* (2018). arXiv: 1811.06965.
- [Ise+22] A. Isenko, R. Mayer, J. Jedelev, and H.-A. Jacobsen. "Where Is My Training Bottleneck? Hidden Trade-Offs in Deep Learning Preprocessing Pipelines." In: *Proceedings of the 2022 International Conference on Management of Data*. SIGMOD '22. Philadelphia, PA, USA: Association for Computing Machinery, 2022, pp. 1825–1839. ISBN: 9781450392495. DOI: 10.1145/3514221.3517848.

- [Jac+91] R. A. Jacobs, M. I. Jordan, S. J. Nowlan, and G. E. Hinton. "Adaptive Mixtures of Local Experts." In: *Neural Computation* 3.1 (1991), pp. 79–87. DOI: 10.1162/neco.1991.3.1.79.
- [KB14] D. P. Kingma and J. Ba. *Adam: A Method for Stochastic Optimization*. 2014. DOI: 10.48550/ARXIV.1412.6980.
- [Kes+16] N. S. Keskar, D. Mudigere, J. Nocedal, M. Smelyanskiy, and P. T. P. Tang. "On Large-Batch Training for Deep Learning: Generalization Gap and Sharp Minima." In: *CoRR* abs/1609.04836 (2016). arXiv: 1609.04836.
- [Kri14] A. Krizhevsky. "One weird trick for parallelizing convolutional neural networks." In: *CoRR* abs/1404.5997 (2014). arXiv: 1404.5997.
- [KSH12] A. Krizhevsky, I. Sutskever, and G. E. Hinton. "ImageNet Classification with Deep Convolutional Neural Networks." In: *Advances in Neural Information Processing Systems*. Ed. by F. Pereira, C. J. C. Burges, L. Bottou, and K. Q. Weinberger. Vol. 25. Curran Associates, Inc., 2012.
- [KW52] J. Kiefer and J. Wolfowitz. "Stochastic Estimation of the Maximum of a Regression Function." In: *The Annals of Mathematical Statistics* 23.3 (1952), pp. 462–466. DOI: 10.1214/aoms/1177729392.
- [Lec+22] G. Leclerc, A. Ilyas, L. Engstrom, S. M. Park, H. Salman, and A. Madry. *ffcv*. <https://github.com/libffcv/ffcv/>. commit xxxxxxxx. 2022.
- [Li+14a] M. Li, D. G. Andersen, A. J. Smola, and K. Yu. "Communication Efficient Distributed Machine Learning with the Parameter Server." In: *Advances in Neural Information Processing Systems*. Ed. by Z. Ghahramani, M. Welling, C. Cortes, N. Lawrence, and K. Weinberger. Vol. 27. Curran Associates, Inc., 2014.
- [Li+14b] M. Li, D. G. Andersen, J. W. Park, A. J. Smola, A. Ahmed, V. Josifovski, J. Long, E. J. Shekita, and B.-Y. Su. "Scaling Distributed Machine Learning with the Parameter Server." In: *Proceedings of the 11th USENIX Conference on Operating Systems Design and Implementation*. OSDI'14. Broomfield, CO: USENIX Association, 2014, pp. 583–598. ISBN: 9781931971164.
- [Li+19a] Q. Li, Z. Wen, Z. Wu, S. Hu, N. Wang, X. Liu, and B. He. "A Survey on Federated Learning Systems: Vision, Hype and Reality for Data Privacy and Protection." In: *CoRR* abs/1907.09693 (2019). arXiv: 1907.09693.
- [Li+19b] Q. Li, Z. Wen, Z. Wu, S. Hu, N. Wang, X. Liu, and B. He. "A Survey on Federated Learning Systems: Vision, Hype and Reality for Data Privacy and Protection." In: *CoRR* abs/1907.09693 (2019). arXiv: 1907.09693.

- [LTJ20] N. Lee, P. H. S. Torr, and M. Jaggi. "Data Parallelism in Training Sparse Neural Networks." In: *CoRR* abs/2003.11316 (2020). arXiv: 2003.11316.
- [MCA19] J. Á. Morell, A. Camero, and E. Alba. "JSDoop and TensorFlow.js: Volunteer Distributed Web Browser-Based Neural Network Training." In: *IEEE Access* 7 (2019), pp. 158671–158684. doi: 10.1109/ACCESS.2019.2950287.
- [Mic20] Microsoft. *Turing-NLG: A 17-billion-parameter language model by Microsoft - Microsoft Research*. <https://www.microsoft.com/en-us/research/blog/turing-nlg-a-17-billion-parameter-language-model-by-microsoft/>. May 2020.
- [Pet+18] M. E. Peters, M. Neumann, M. Iyyer, M. Gardner, C. Clark, K. Lee, and L. Zettlemoyer. "Deep contextualized word representations." In: *CoRR* abs/1802.05365 (2018). arXiv: 1802.05365.
- [Rad+19] A. Radford, J. Wu, R. Child, D. Luan, D. Amodei, and I. Sutskever. "Language Models are Unsupervised Multitask Learners." In: (2019).
- [Raf+19] C. Raffel, N. Shazeer, A. Roberts, K. Lee, S. Narang, M. Matena, Y. Zhou, W. Li, and P. J. Liu. "Exploring the Limits of Transfer Learning with a Unified Text-to-Text Transformer." In: *CoRR* abs/1910.10683 (2019). arXiv: 1910.10683.
- [Ram+21] A. Ramesh, M. Pavlov, G. Goh, S. Gray, C. Voss, A. Radford, M. Chen, and I. Sutskever. "Zero-Shot Text-to-Image Generation." In: *CoRR* abs/2102.12092 (2021). arXiv: 2102.12092.
- [RG] M. Ryabinin and A. Gusev. *learning@home*. <https://learning-at-home.github.io/>.
- [RG20a] M. Riabinin and A. Gusev. "Learning@home: Crowdsourced Training of Large Neural Networks using Decentralized Mixture-of-Experts." In: *CoRR* abs/2002.04013 (2020). arXiv: 2002.04013.
- [RG20b] M. Riabinin and A. Gusev. "Learning@home: Crowdsourced Training of Large Neural Networks using Decentralized Mixture-of-Experts." In: *CoRR* abs/2002.04013 (2020). arXiv: 2002.04013.
- [Rya+21a] M. Ryabinin, E. Gorbunov, V. Plokhotnyuk, and G. Pekhimenko. "Moshpit SGD: Communication-Efficient Decentralized Training on Heterogeneous Unreliable Devices." In: *CoRR* abs/2103.03239 (2021). arXiv: 2103.03239.
- [Rya+21b] M. Ryabinin, E. Gorbunov, V. Plokhotnyuk, and G. Pekhimenko. "Moshpit SGD: Communication-Efficient Decentralized Training on Heterogeneous Unreliable Devices." In: *CoRR* abs/2103.03239 (2021). arXiv: 2103.03239.

- [Sha+18] C. J. Shallue, J. Lee, J. M. Antognini, J. Sohl-Dickstein, R. Frostig, and G. E. Dahl. “Measuring the Effects of Data Parallelism on Neural Network Training.” In: *CoRR* abs/1811.03600 (2018). arXiv: 1811.03600.
- [Sho+19] M. Shoeybi, M. Patwary, R. Puri, P. LeGresley, J. Casper, and B. Catanzaro. “Megatron-LM: Training Multi-Billion Parameter Language Models Using Model Parallelism.” In: *CoRR* abs/1909.08053 (2019). arXiv: 1909.08053.
- [Smi+22] S. Smith, M. Patwary, B. Norick, P. LeGresley, S. Rajbhandari, J. Casper, Z. Liu, S. Prabhunoye, G. Zerveas, V. Korthikanti, E. Zheng, R. Child, R. Y. Aminabadi, J. Bernauer, X. Song, M. Shoeybi, Y. He, M. Houston, S. Tiwary, and B. Catanzaro. “Using DeepSpeed and Megatron to Train Megatron-Turing NLG 530B, A Large-Scale Generative Language Model.” In: *CoRR* abs/2201.11990 (2022). arXiv: 2201.11990.
- [SZ14] K. Simonyan and A. Zisserman. *Very Deep Convolutional Networks for Large-Scale Image Recognition*. 2014. DOI: 10.48550/ARXIV.1409.1556.
- [tea20] L. team. *Hivemind: a Library for Decentralized Deep Learning*. <https://github.com/learning-at-home/hivemind>. 2020.
- [Xin+21] D. Xin, H. Miao, A. Parameswaran, and N. Polyzotis. “Production Machine Learning Pipelines: Empirical Analysis and Optimization Opportunities.” In: *Proceedings of the 2021 International Conference on Management of Data*. SIGMOD ’21. Virtual Event, China: Association for Computing Machinery, 2021, pp. 2639–2652. ISBN: 9781450383431. DOI: 10.1145/3448016.3457566.
- [XRV17] H. Xiao, K. Rasul, and R. Vollgraf. “Fashion-MNIST: a Novel Image Dataset for Benchmarking Machine Learning Algorithms.” In: *CoRR* abs/1708.07747 (2017). arXiv: 1708.07747.
- [YGG17] Y. You, I. Gitman, and B. Ginsburg. “Scaling SGD Batch Size to 32K for ImageNet Training.” In: *CoRR* abs/1708.03888 (2017). arXiv: 1708.03888.
- [You+19] Y. You, J. Li, J. Hseu, X. Song, J. Demmel, and C.-J. Hsieh. “Reducing BERT Pre-Training Time from 3 Days to 76 Minutes.” In: *CoRR* abs/1904.00962 (2019). arXiv: 1904.00962.
- [Zha+20] Z. Zhang, C. Chang, H. Lin, Y. Wang, R. Arora, and X. Jin. “Is Network the Bottleneck of Distributed Training?” In: *CoRR* abs/2006.10103 (2020). arXiv: 2006.10103.